

Domoic Acid as a Lead for the Discovery of the First Selective Ligand for Kainate Receptor Subtype 5 (GluK5)

Silke Buschbom-Helmke, Pengfei Wang, Anna Alcaide, Federico Miguez-Cabello, Mario Carta, Julio S. Viotti, Birgitte Nielsen, Christophe Mulle, Derek Bowie, Flemming Steen Jørgensen, Darryl S. Pickering, and Lennart Bunch*



Cite This: *J. Med. Chem.* 2024, 67, 14524–14542



Read Online

ACCESS |



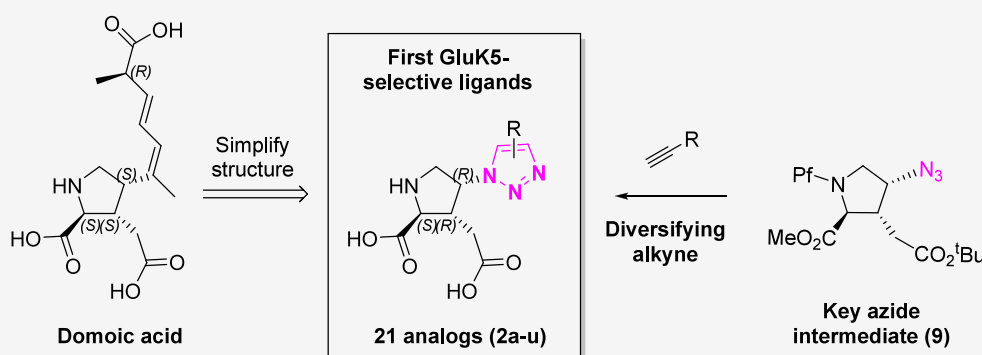
Metrics & More



Article Recommendations



Supporting Information



ABSTRACT: Twenty-one simplified analogues of the natural product domoic acid were designed, synthesized, and then characterized at homomeric kainic acid (KA) receptors (GluK1-3,5). **LBG20304** displays a high affinity for homomeric GluK5 receptors ($IC_{50} = 432$ nM) with a >40-fold selectivity over homomeric GluK1-3 subtypes and $\gg 100$ -fold selectivity over native AMPA and *N*-methyl *D*-aspartate receptors. Functional studies of **LBG20304** on heteromeric GluK2/5 receptors show no agonist or antagonist functional response at 10 μ M, while a concentration of 100 μ M at neuronal slices (rat) shows low agonist activity. A molecular dynamics simulation of **LBG20304**, in a homology model of GluK5, suggests specific interactions with the GluK5 receptor and an occluded ligand binding domain, which is translated to agonist or partial agonist activity. **LBG20304** is a new compound for the study of the role and function of the KA receptors with the aim of understanding the involvement of these receptors in health and disease.

INTRODUCTION

Glutamate (Glu) receptors continue to be an important field of study for understanding neurological mechanisms underlying the healthy and diseased brain. Glu receptors are divided into ionotropic Glu receptors (iGluRs, ion channels) and metabotropic Glu receptors (mGluRs, G-protein coupled). Based on sequence similarity and agonist selectivity studies, the iGluRs are further divided into the three groups α -amino-3-hydroxy-5-methyl-4-isoxazolepropionic acid (AMPA), kainic acid (KA), and *N*-methyl-*D*-aspartate (NMDA) receptors.¹ Here we focus on the KA receptors, which form functional receptors from homomeric or heteromeric combinations of four GluK1-3 subunits (dimer of dimers), whereas the GluK4,5 subunits only form functional receptors in combination with GluK1-3 subunits (also as dimer of dimers).²

Extensive effort has been made to discover tool compounds for the KA receptors, however, with limited success: Selective agonists,³ antagonists^{4,5} and one selective negative allosteric modulator (NAM)⁶ have been reported for homomeric GluK1

receptors, and recently the first selective agonist^{7,8} and antagonist⁹ for homomeric GluK3 receptors were disclosed. X-ray structures of the ligand binding domains of GluK1-3 (GluK1-LBD, GluK2-LBD and GluK3-LBD) in complex with a vast number of ligands have been determined, and this comprehensive work provided insights into the correlation between degree of LBD domain closure and ligand agonist/antagonist function.¹⁰ Recent advances in structural biology have led to cryo-EM structures of full-length homomeric GluK2¹¹ and heteromeric GluK2/K5² receptors. In summary, the field is moving forward but is nevertheless characterized with

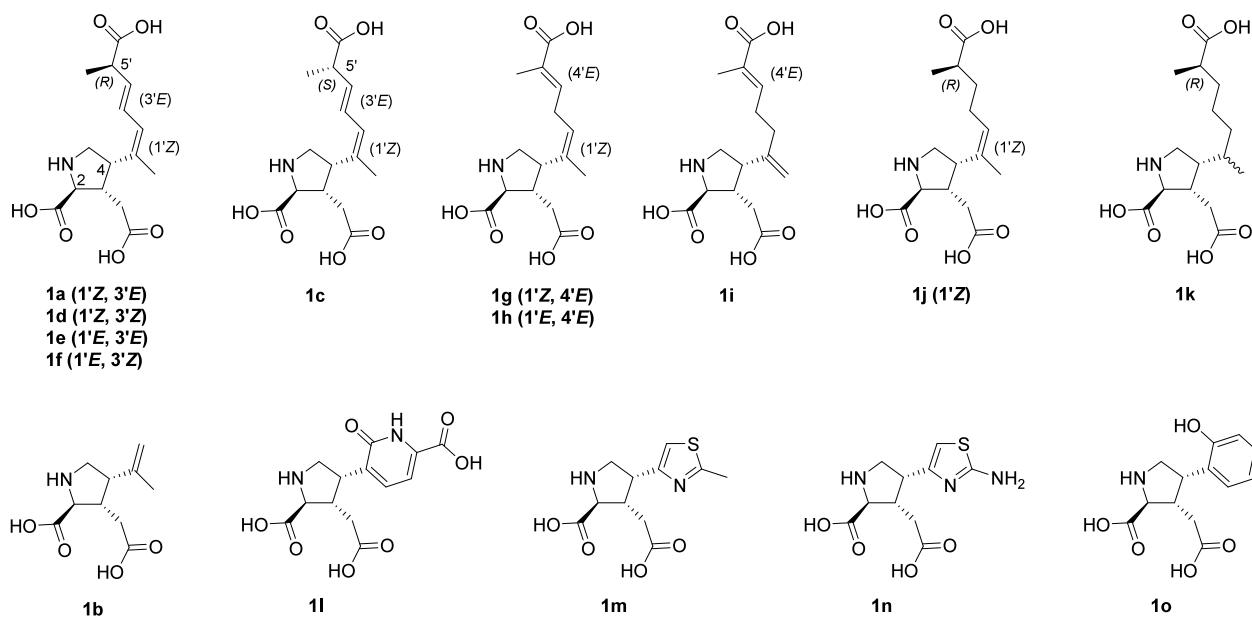
Received: June 10, 2024

Revised: July 18, 2024

Accepted: July 23, 2024

Published: August 12, 2024



Table 1. Binding Affinities of Naturally Occurring and Synthetic Kainoids at Native AMPA, KA, and NMDA Receptors (rat synaptosomes)

compound	acronym	native receptors (rat synaptosomes) [IC ₅₀ (nM)]		cloned homomeric receptors [K _i in (nM)]			
		AMPA	KA	GluK1 ^b	GluK2 ^b	GluK3 ^b	CA1 slice
1a ^{13,16}	DA	470, ^c 9000	4, ^c 15	1.11	6.04	4.84	228
1b ¹⁶	KA	1900	12	— ^e	— ^e	— ^e	— ^e
1c ¹⁷	(S'S)-DA	5700	28	— ^e	— ^e	— ^e	— ^e
1d ¹⁷	DA-D	17000	28	— ^e	— ^e	— ^e	— ^e
1e ¹⁷	DA-E	12000	940	— ^e	— ^e	— ^e	— ^e
1f ¹⁷	DA-F	32000	1400	— ^e	— ^e	— ^e	— ^e
1g ¹⁴	DA-A	— ^e	— ^e	— ^e	130	— ^e	887
1h ¹⁷	DA-B	— ^e	— ^e	— ^e	— ^e	— ^e	— ^e
1i ¹⁴	DA-C	— ^e	— ^e	— ^e	— ^e	— ^e	3,712
1j ¹⁷	DH-DA-D	3600	9	— ^e	— ^e	— ^e	— ^e
1k ¹⁷	TH-DA ^d	>100000	27000	— ^e	— ^e	— ^e	— ^e
1l ¹⁶	ACRO-A	60	330	— ^e	— ^e	— ^e	— ^e
1m ¹⁵	— ^e	— ^e	6	— ^e	— ^e	— ^e	— ^e
1n ¹⁵	— ^e	— ^e	5	— ^e	— ^e	— ^e	— ^e
1o ¹⁶	— ^e	130	5.8	— ^e	— ^e	— ^e	— ^e

^aFor the sake of clarity, all values are rounded off. ^bRadioligand [³H](2S,4R)-4-MeGlu (SYM-2081). ^cRat spinal cord synaptosomes were used.

^dMixture of C1' stereoisomers. ^eNo data available.

a striking need for the disclosure of novel tool compounds with unprecedented subunit and/or subtype selectivity profiles.

The natural product domoic acid (DA, **1a**) (Table 1), first isolated from the red marine alga *Chondria armata* in 1958,¹² and its analogues (**1c–k**) (Table 1) comprise an (S)-proline core bearing a 2,3-*trans*-3-carboxymethyl substituent and a chemically enriched and diversified side chain in the 4-position detained in a 3,4-*cis* relationship. The compound class shares structural features with the receptor group defining natural product KA (**1b**), differing only by truncation of the 4-substituent to an *iso*-propylene group (Table 1). **1a** is highly neurotoxic and displays selective low nanomolar affinity for native KA receptors and cloned homomeric subtypes GluK1–3.¹³ Furthermore, in hippocampal slices, **1a** was shown to be a full agonist (EC₅₀ = 228 nM).¹⁴

A number of regio- and/or stereoisomers of **1a** have also been isolated (Table 1): The C5'-epimer **1c**,⁹⁶ and the 3',4'-Z-stereoisomer **1d**, both show similar binding affinities for native

KA receptors. On the other hand, the 1',3'-*E*-configuration leads to a dramatic drop in binding affinity (analogues **1e** and **1f**). Shifting the 3',4'-alkene to the 4',5' position (analogue **1g**) results in a ~ 20-fold lower binding affinity to GluK2, but it remains a full agonist in CA1 slices with an only 4-fold drop in EC₅₀ value (EC₅₀ = 887 nM). In contrast, **1i** displays significantly reduced activity in CA1 slices (EC₅₀ = 3,712 nM). Synthetic analogues of **1a** comprise the 3',4'-dihydro analogue **1j**, which display a ~ 2-fold increase in binding affinity for native KA receptors. The 1',2',3',4'-tetrahydro analogue **1k**, however, led to a complete loss in affinity for native KA receptors. The latter finding correlates very well with the fact that also the 1',2'-dihydro analogue of **1b** (dihydrokainic acid, not shown) is also a low-affinity ligand for native KA receptors.

In summary the structure–activity relationship (SAR) of **1a** and its natural and synthetic analogues can be condensed to (a) C1' geometry must be sp²-hybridized, (b) the stereochemistry

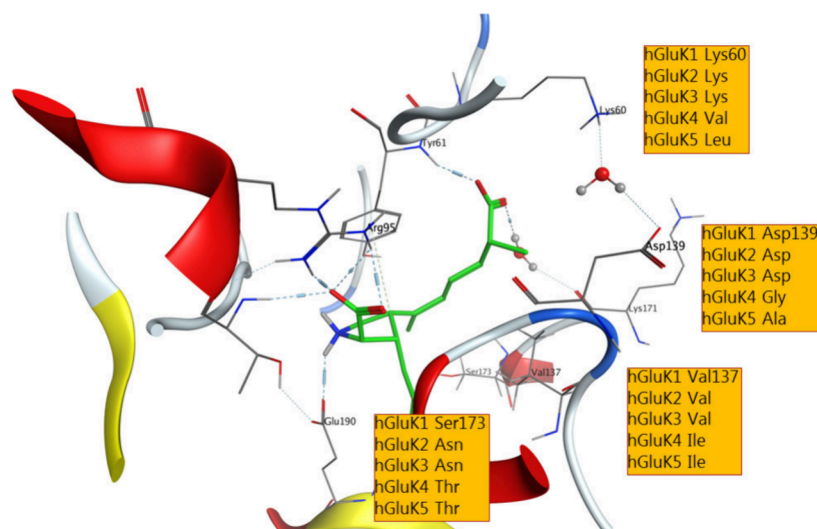
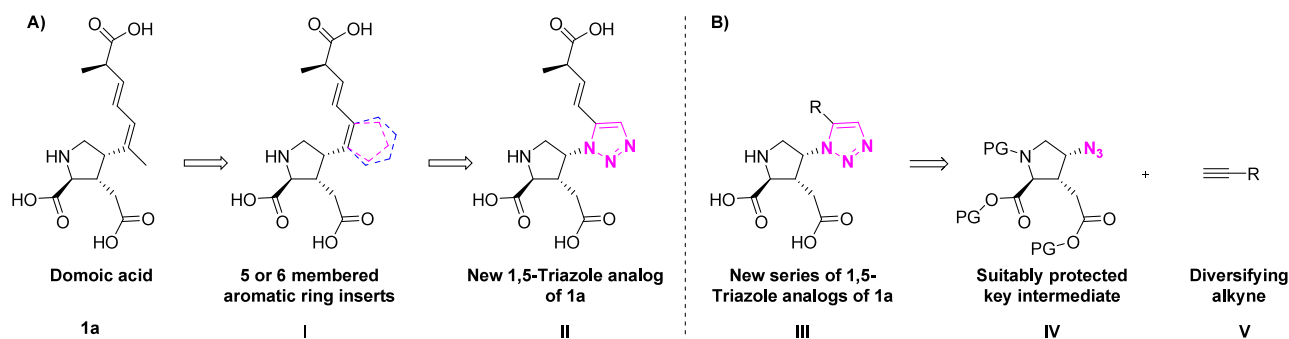


Figure 1. X-ray structure of GluK1-LBD crystallized with DA (**1a**) (PDB entry 2PBW).¹⁸ Residues that are different between GluK1 and GluK2-5 are highlighted in the orange boxes.

Scheme 1. (A) Design Strategy for a Structurally Simplified Five-Membered Heteroaromatic Ring (purple) or Six-Membered (Hetero)aromatic Ring (blue) (I) Analogue of **1a** (compound II) and (B) Retrosynthetic Analysis of Generalized Triazole III, Suggesting Azide IV as the Key Intermediate



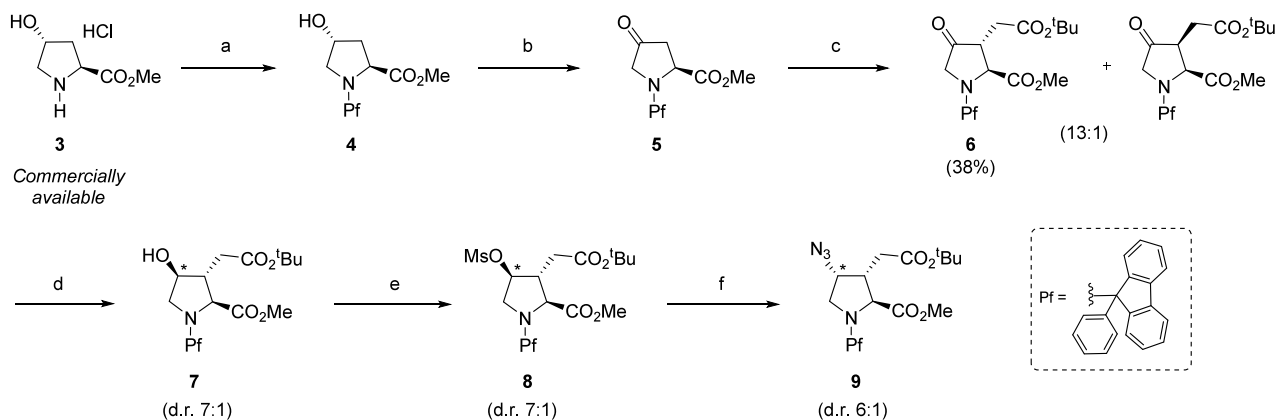
of C5' is of less importance, and (c) the 3',4' alkene is not essential for affinity.

Acromelic acid A (**11**) (Table 1) represents another class of natural products which share structural features of **1a** and **1b**, but comprise a planar heterocycle directly attached to the C4 position of the proline ring. **11** displays midrange nanomolar affinity for native KA receptors (330 nM), but a ~5-fold higher affinity for AMPA receptors. The synthetic analogues **1m** and **1n** comprise a smaller in size five-membered planar heterocycle in the C4 position and both display low nanomolar affinity for native KA receptors. Regrettably, affinities for AMPA receptors were not reported. Also, phenyl analogue **1o** displays low nanomolar affinity for KA receptors with ~20-fold selectivity over AMPA receptors.¹⁵

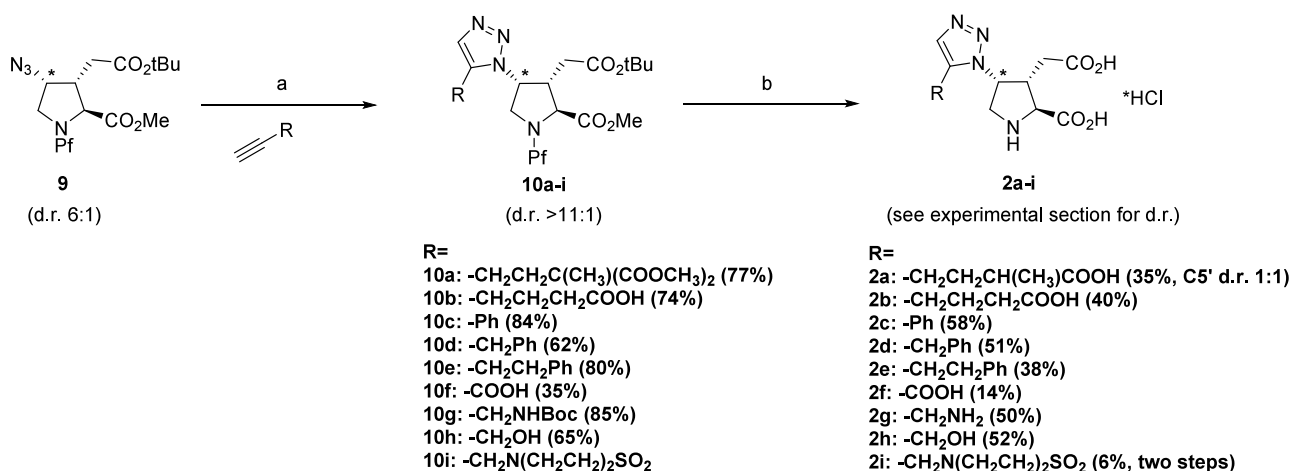
X-ray. X-ray structures of **1a** have been obtained when bound to the GluK1- and GluK2-ligand binding domains (GluK1-LBD, PDB entry 2PBW¹⁸ and GluK2-LBD, PDB entry 1YAE¹⁹) (Figure 1). In both structures, the 4-position side chain reaches into a highly hydrophilic and water rich area, with the terminal C6' carboxylate group engaged in hydrogen bond interactions with backbone NH of Tyr61 (GluK1 numbering) and via a bridging water molecule to backbone carbonyl group of Lys171 (GluK1 numbering). The domain closure was calculated to be 67% and 46%, respectively, suggesting that **1a** is a partial agonist

at GluK1¹⁸ and GluK2.¹⁹ This is intriguing since **1a** is reported as a full agonist in CA1 slices.¹⁴

With the aim to discover novel tool compounds for the KA receptors, which possess a distinct and novel selectivity profile, we saw **1a** as an attractive lead due to its broad and high-affinity profile among the KA receptor subtypes and its selectivity over native AMPA and NMDA receptors (Table 1). On the examination of its binding mode in GluK1-LBD (Figure 1), we noticed that the C4-side chain reaches into an area of the GluK1 receptor, which contains differentiated residues across the GluK1–5 subunits: In details, the basic residue Lys60 (GluK1) engages in a salt bridge with the distal carboxylate group of Asp139 (GluK1) via a water molecule. This salt-bridge interaction is conserved in GluK2 and GluK3, but in GluK4 and GluK5 the basic residue Lys60 (GluK1) is replaced by the neutral and lipophilic amino acids Val and Leu, and the acidic residue Asp139 is replaced by Gly and Ala, respectively. On these grounds, we hypothesized that disruption of the water matrix in GluK1-3 is more costly (tightly bound waters), compared to GluK4,5. Thus, by replacing the terminal C4-carboxylate group in **1a** with a lipophilic functionality, selectivity for GluK4 and/or GluK5 could be obtained.

Scheme 2. Synthesis of Key Azide Intermediate 9 from Commercially Available Proline Analogue 3^{4a}

^aReagents and conditions: (a) Pf-Br, Et₃N, CH₂Cl₂, 0 °C to rt, (71%); (b) Dess-Martin periodinane, CH₂Cl₂, overnight, (72%); (c) *tert*-butyl bromoacetate, *n*-BuLi, NaI, HMPA, THF (38%, 13:1); (d) NaBH₄, CH₃OH (65%, d.r. 7:1); (e) MsCl, Et₃N, CH₂Cl₂, 0 °C to rt, (57%); (f) NaN₃, DMPU, DMF, 80 °C (74%).

Scheme 3. Synthesis of Triazole Analogues 2a–i from Key Azide 9^{4a}

^aReactions and conditions: (a) alkyne, Cp^{*}RuCl(PPh₃)₂, THF, microwave oven, 100 °C, 2 h (35–85%); (b) 6 M HCl (aq), reflux, overnight (14–58%).

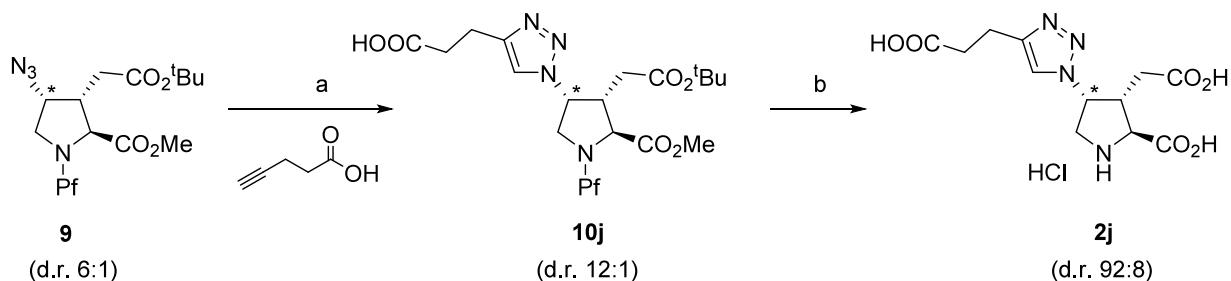
RESULTS AND DISCUSSION

Natural product **1a** is a chemically complex proline analogue comprising four stereocenters, two stereospecific alkenes, and four polar functional groups. For our redesign, we thus sought to reduce the chemical complexity to a scaffold which would allow for the expedited synthesis of analogues comprising variations of the C4-side chains for an expansive SAR study. Given the insights from SAR studies of **1a** and its reported natural and synthetic analogues, we decided to replace the 2',3'-alkene with a planar 5- or 6-membered cyclic ring (**I**, Scheme 1). Based on computational studies addressing low-energy conformation, binding mode, ligand size/bulk, pocket space and considerations of synthetic tractability, we decided on incorporation of a triazole ring with a 1,5-substitution pattern (**II**, Scheme 1). This design allowed for the use of azide intermediate **IV** (Scheme 1) for late stage diversification (**III**, Scheme 1).

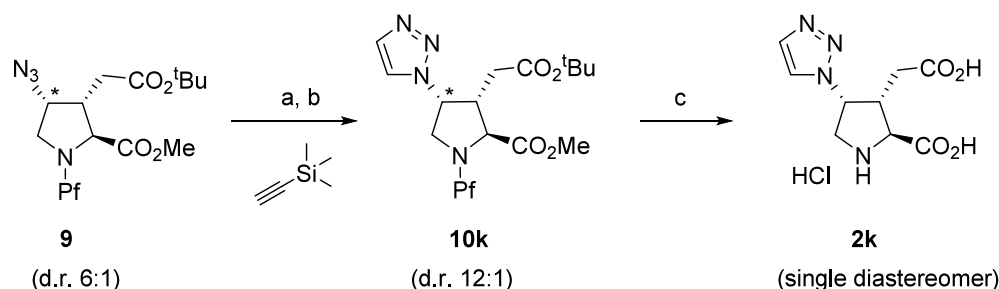
Chemistry. Regioselective alkylation of the 3-position in 4-oxo prolines can be achieved by protection of the amino group with the 9-phenyl-9H-fluoren-9-yl (Pf) group.²⁰ The stereochemical outcome is directed by the configuration at the 2-position to give a 2,3-*trans* relationship as the predominant diastereomer. Thus, starting from commercially available methyl

(2*S*,4*R*)-4-hydroxypyrrolidine-2-carboxylate hydrochloride (**3**) (Scheme 2), the amine was first protected by reaction with 9-bromo-9-phenylfluorene (Pf-Br) in the presence of triethylamine (TEA) to give **4** in a 71% yield. The alcohol was oxidized to its corresponding ketone **5** under standard Dess-Martin oxidation conditions. Regioselective alkylation at position 3 with *tert*-butyl 2-bromoacetate proceeded smoothly in accordance with literature precedents,²¹ giving intermediate **6** in moderate 38% yield, as a single diastereomer after purification. Hydride reduction of the ketone afforded alcohol **7** as a mixture of diastereomers (d.r. 7:1), which was in contrast to the previous report on this reaction being fully diastereoselective.²¹ All attempts to improve the diastereoselectivity were unsuccessful. Next, the alcohol group was transformed into its mesylate **8**, which was subsequently reacted with sodium azide in DMPU to give key azide intermediate **9** in 43% (d.r. 6:1) over 2 steps.

To access the series of 1,5-substituted triazoles **2a–i**, we applied the ruthenium catalyzed azide alkyne cycloaddition (RuAAC) reaction using Cp^{*}RuCl(PPh₂)₃ as catalyst (Scheme 3). In accordance with reported conditions we used 5 mol % Cp^{*}RuCl(PPh₃)₂ and phenylpropyne **10d** in dioxane at 60 °C.²² However, no conversion was obtained after 24 h, and even

Scheme 4. Synthesis of 2j as the 1,4-Regioisomer of DA Analogue 2b from Key Azide Intermediate 9^a

^aReactions and conditions: (a) alkyne, CuI, DMF:MeOH (9:1), 90 °C, overnight (59%); (b) 6 M HCl (aq), reflux, overnight (56%).

Scheme 5. Synthesis of Free Triazole 2k from Key Azide 9^a

^aReactions and conditions: (a) trimethylsilylethyne, CuI, DMF:MeOH (9:1), 90 °C, 4 days; (b) 1 M TBAF, rt, overnight (59%, two steps); (c) 6 M HCl (aq), reflux, overnight (47%).

Table 2. Binding Affinities of 2a–k at Native AMPA, KA, and NMDA Receptors (rat synaptosomes) and Cloned Homomeric Receptors GluK1–3,^a

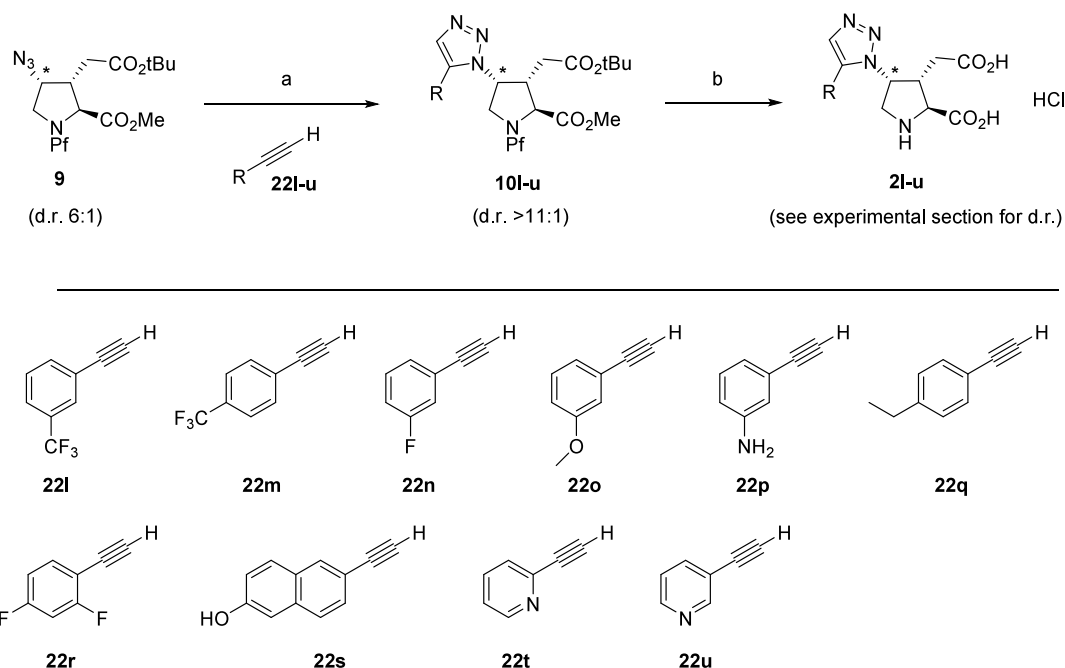
compound	R	AMPA ^{b,d}	KA ^{b,d}	NMDA ^{c,d}	GluK1 ^{c,d}	GluK2 ^{c,d}	GluK3 ^{c,d}	GluK5 ^{c,d}
2a	triazole DA analogue	(73 ± 6)	1.73 ± 0.07	(102 ± 5)	11.7 ± 5.8	8.66 ± 0.60	5.90 ± 0.91	0.420 ± 0.160
2b	desmethyl DA analogue	(86 ± 2)	2.30 ± 0.40	(90 ± 3)	10.8 ± 3.4	7.79 ± 0.36	6.10 ± 1.95	0.483 ± 0.136
2c	Ph-	(80 ± 6)	5.10 ± 0.36	(101 ± 3)	(93 ± 2)	36 ± 6	21.1 ± 3.8	0.499 ± 0.068
2d	PhCH ₂ -	(86 ± 4)	(79 ± 11)	(87 ± 7)	(99 ± 3)	(92 ± 10)	(94 ± 13)	11.1 ± 4.8
2e	PhCH ₂ CH-	(98 ± 4)	35 ± 2	(98 ± 9)	(94 ± 3)	(97 ± 16)	(90 ± 15)	5.57 ± 2.82
2f	HOOC-	(85 ± 14)	(80 ± 9)	(66 ± 13)	(79 ± 4)	(85 ± 13)	(79 ± 5)	(85 ± 4)
2g	NH ₂ CH ₂ -	(100 ± 2)	(76 ± 13)	(92 ± 14)	(95 ± 1)	(79 ± 4)	(81 ± 15)	(85 ± 8)
2h	HOCH ₂ -	(86 ± 14)	22 ± 1	(102 ± 10)	(94 ± 2)	(76 ± 5)	(84 ± 15)	7.97 ± 1.49
2i	R' ₂ NCH ₂ -	– ^e	– ^e	– ^e	(97.0 ± 0.4)	(80 ± 13)	(91 ± 1)	(94 ± 9)
2j	4' regioisomer	>100	>100	>100	>100	>100	>100	– ^e
2k	H	9.5 ± 0.7	1.3 ± 0.1	>100	3.3 ± 0.04	2.6 ± 0.31	0.28 ± 0.02	– ^e

^aFor the chemical structure of the R group, see Scheme 3. ^bIC₅₀ values in μM (mean ± SEM). ^cK_i values in μM (mean ± SEM). ^dIn parentheses are shown the percent binding values of the radioligand at 10 μM ligand (mean value ± standard deviation). ^eNot tested.

heating to 100 °C with prolonged reaction time only resulted in traces of product 10d. Based on the work of Pradere et al. with other secondary azides²³ microwave conditions were applied with small modification: Catalyst loading was increased to 10 mol % and reaction time extended to 2 h. Under these conditions, irradiation at 100 °C in THF resulted in full consumption of azide 9 and the formation of product 10d in 62%. With these conditions in hand, intermediates 10a–i were obtained in moderate to good yields and with improved diastereo ratios after purification (35–85%, d.r. > 11:1). Global deprotection was carried out with 6 M HCl at reflux for 6 h to give target products 2a–i after preparative HPLC in 6–58% yield (d.r. determined by ¹H NMR and/or HPLC). It was noted that *tert*-butylation of the final product was a competing reaction if performed in closed vials. Dilution to 10 mL 6 M HCl and fitting the flask with a reflux condenser circumvented this problem.

For the synthesis of the 1,4-regioisomeric analogue 2j (Scheme 4), azide precursor 9 was first reacted with 4-pentynoic acid using CuI in DMF-MeOH 9:1 at 90 °C (CuACC conditions), to give propanoic acid 10j in a modest 59% yield, exclusively as the 1,4-regioisomer. Deprotection of the amine was carried out in 6 M aq HCl at reflux to afford the 2j in 56% yield.

Unsubstituted triazole 2k (Scheme 5) was also prepared using the CuACC reaction conditions starting from azide 9, and trimethylsilylethyne as the alkyne. The crude product was a mixture of 10k together with its 4'-TMS analogue, which was treated directly with *tetra-N*-butylammonium fluoride (TBAF) in THF to afford 10k in 59% yield, over two steps. Subsequent treatment with 6 M aq HCl at reflux gave target compound 2k in 47% yield.

Scheme 6. Synthesis of Triazole Analogues 2l–u from Key Azide 9 and In House Available Alkynes 22l–u^a

^aReactions and conditions: (a) alkyne, Cp*₂RuCl(PPh₃)₂, THF, microwave oven, 100 °C, 2 h; (b) 6 M HCl (aq), reflux, overnight.

Table 3. Binding Affinities of 2l–u at Native AMPA, KA, and NMDA Receptors (rat synaptosomes) and Cloned Homomeric Receptors GluK1-3,5

compound	R	AMPA ^c	KA ^a	NMDA ^c	GluK1 ^{b,c}	GluK2 ^{b,c}	GluK3 ^{b,c}	GluK5 ^{b,c}
2c	Ph-	(80 ± 6)	5.1 ± 0.4	(101 ± 3)	(93 ± 2)	36 ± 6	21.1 ± 3.8	0.499 ± 0.068
2l	<i>m</i> -CF ₃ Ph-	– ^d	– ^d	– ^d	(92 ± 3)	(76 ± 7)	(90 ± 11)	2.15 ± 0.91
2m	<i>p</i> -CF ₃ Ph-	– ^d	– ^d	– ^d	(95 ± 3)	(103 ± 8)	(85 ± 3)	(62 ± 7)
2n	<i>m</i> -F-Ph-	– ^d	– ^d	– ^d	(60 ± 22)	(76 ± 1)	(58 ± 4)	1.76 ± 0.24
2o	<i>m</i> -CH ₃ O-Ph-	– ^d	– ^d	– ^d	(88 ± 5)	(89 ± 3)	(74 ± 6)	1.02 ± 0.24
2p	<i>m</i> -NH ₂ Ph-	– ^d	– ^d	– ^d	(97 ± 2)	(102 ± 12)	(93 ± 9)	3.25 ± 1.56
2q	<i>p</i> -Et-Ph-	– ^d	– ^d	– ^d	(95 ± 6)	(92 ± 3)	(83 ± 2)	(45 ± 12)
2r	<i>o,p</i> -DiF-Ph-	– ^d	– ^d	– ^d	(96 ± 1)	(73 ± 3)	(90 ± 8)	5.35 ± 1.95
2s (LBG20304)	6-HO-naphth-2-yl-	(90 ± 7)	4.4 ± 0.7	(99 ± 14)	(90 ± 0.1)	70 ± 12	17.9 ± 3.2	0.432 ± 0.089
2t	2-pyridyl	– ^d	– ^d	– ^d	11.5 ± 1.2	7.76 ± 5.53	3.75 ± 1.46	0.258 ± 0.057
2u	3-pyridyl	– ^d	– ^d	– ^d	(98 ± 6)	(92 ± 6)	(80 ± 5)	(47 ± 7)

^aIC₅₀ values in μM (mean ± SEM). ^bK_i values in μM (mean ± SEM). ^cIn parentheses are shown the percent binding values of the radioligand at 10 μM ligand (mean value ± standard deviation). ^dNot tested.

PHARMACOLOGY

Triazole analogues 2a–k were characterized in binding at native AMPA, KA and NMDA receptors (rat synaptosomes) and homomeric GluK1-3,5 receptors (Table 2). DA analogue 2a preserved KA selectivity over AMPA and NMDA receptors and interestingly already displayed preference (14–28-fold) for GluK5 over GluK1-3, but, affinity was generally reduced compared to 1a. The affinity profile of demethyl DA analogue 2b was comparable with 2a, which was in line with 1a versus 1c. For the three lipophilic analogues 2c (Ph-), 2d (PhCH₂-) and 2e (PhCH₂CH₂-), 2c was the most prominent with high nanomolar affinity (0.5 μM) for GluK5 and >40-fold selectivity over GluK1-3. Extending the distance between the Ph and triazole rings by incorporation of a methylene linker (2d), or an ethylene linker (2e) led to a 10–20-fold reduction in binding affinity for GluK5, but selectivity over GluK1-3 was interestingly preserved.

The charged hydrophilic analogues 2f (–COOH) and 2g (–CH₂NH₂) led to a complete loss of affinity for all KA receptors, whereas alcohol 2h (–CH₂OH) was selective for GluK5, however with 15-fold reduced affinity compared to best analogue so far 2c. Sulfone 2i was without affinity to any of GluK1-3,5 subtypes. DA regioisomer 2j was as expected also without affinity for any of the iGluRs, while free triazole 2k showed a broader affinity profile across the iGluRs.

Second SAR Round. With the finding, that 5-phenyl analogue 2c displays selective binding at homomeric GluK5 over GluK1-3 and native GluRs, we decided to continue our SAR study by exploring the impact of substituents on the phenyl ring. We synthesized a total of 10 analogues, based on already available alkynes 22l–u and the available quantity of azide 9. The analogues were comprised of substituents in the *meta* and *para* positions 2l–q, ortho/*para* 2r, but also substituting the phenyl ring for a hydroxynaphthyl 2s as well as for 2- and 3-pyridyl rings 2t,u (Scheme 6). The two-step syntheses starting

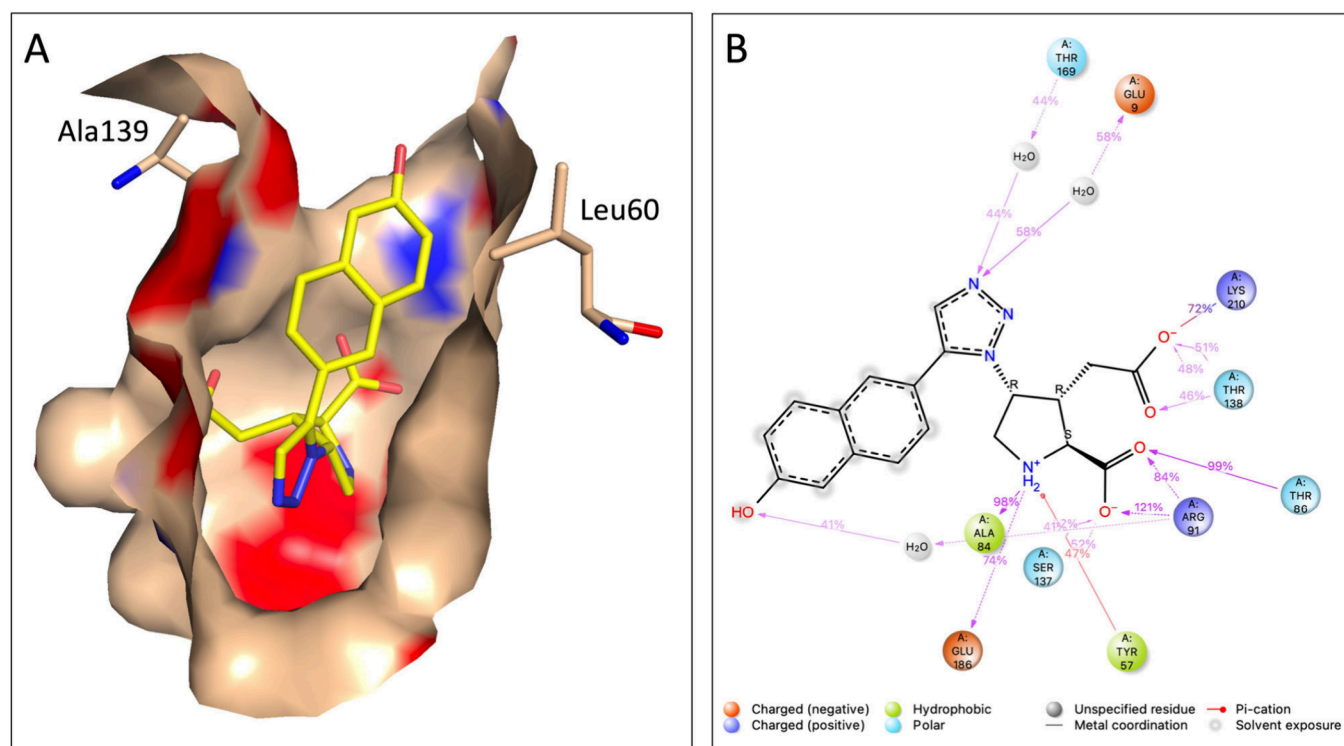


Figure 2. MD simulation of **LBG20304** in a homology model of GluK5-LBD from the GluK1-LBD crystallized with KA (PDB entry 4E0X). (A) Proposed binding mode of **LBG20304** in GluK5 corresponding to the last frame from the MD simulation. Surface of the GluK5 residues closest to **LBG20304** are displayed, and Leu60 and Ala139 are shown as stick models, with oxygens colored red, nitrogens colored blue, and all other atoms colored wheat. The structure of **LBG20304** is shown in the GluK5 cavity as a stick model, with oxygens colored red, nitrogens colored blue, and carbons colored yellow. (B) GluK5-**LBG20304** intermolecular contacts observed during the MD simulation. Only contacts present in >40% of the simulation time are shown.

from azide **9**, were carried out without purification of intermediates **10l–u**.

The target compounds **2l–u** were characterized in binding at homomeric GluK1–3 and GluK5 receptors and results are summarized in Table 3 (an assay expressing homomeric GluK4 is not available at the present time). The SAR study shows that introduction of a trifluoromethyl group in the *meta* or *para* positions (compounds **2l** and **2m**) did not improve the binding affinity for GluK5. The same was observed for fluorine in the *meta* position (**2n**) and also the difluoro analogue **2r** all of which showed reduced affinity for GluK5. When the *meta* position was probed with a methoxy group **2o**, or an aniline functionality **2p**, a 2–7-fold reduction in GluK5 binding was observed. An ethyl group in the *para* position **2q** was clearly not tolerated and led to a ~100-fold reduced affinity for GluK5. In contrast, the hydroxynaphthyl group, analogue **2s** (**LBG20304**), was well-accommodated and its full pharmacological profile showed that the selectivity was slightly improved compared to **2c**. Most interesting, the 2-pyridyl analogue **2t** displayed a 2-fold enhanced affinity for GluK5, but disappointingly, selectivity over GluK1–3 was compromised. In contrast, 3-pyridyl analogue **2u** led to significant loss in affinity for all GluK1–3,5 receptors.

Molecular Dynamics. With the first GluK5 selective ligand in hand, we wanted to address in more detail its binding mode at GluK5-LBD and compare the binding mode of **LBG20304** with DA. For this we constructed a homology model of GluK5-LBD from GluK1-LBD crystallized with KA (PDB entry 4E0X) and subsequently docked **LBG20304** and DA, respectively, in this GluK5-LBD model (Figure 2). We chose this approach over starting from the crystal structure of GluK1 with DA (PDB entry

2PBW), to avoid comparing an experimentally determined binding mode of DA with a modeled binding mode of **LBG20304**. Details on the model building are available in the Supporting Information.

The MD simulations of the **LBG20304** and DA in complex with GluK5-LBD reveal that the protein structure remains constant, and we do not observe any domain opening or further domain closure (Supporting Information, Figure S1–S3). Although distinct domain opening or closure cannot be expected to appear during 1000 ns MD simulations at 300 K, we have previously by similar MD simulations been able to observe differences, which could be correlated with different dynamics of the LBDs of the Glu delta receptors.²⁴

The disruption of the water mediated hydrogen bond between Asp139 and Lys60 present in GluK1 and the mutation of these residues to the hydrophobic residues Leu60 and Ala139 in GluK5 leads to a slightly wider cavity due to the side chains being smaller. The orientation of the naphthalene moiety in **LBG20304** rotates during the MD simulation to gain an optimal fit to the cavity compared to the orientation of the 2,3-*trans*-3-carboxymethyl substituent in DA (Figure 2A). The N3 in the triazole ring and the hydroxy group at the naphthalene rings form water-mediated hydrogen bonds to GluK5 residues Thr169 and Glu9, and the hydroxy group at the naphthalene ring interacts with Arg91 also mediated by water (Figure 2B). In general, **LBG20304** bind analogously to KA and DA in reported crystal structures (PDB entries 1YAE, 2PBW, 4E0X, and 5IKB). Thus, the MD simulations indicate that **LBG20304** binds as designed with the hydrophobic naphthalene moiety

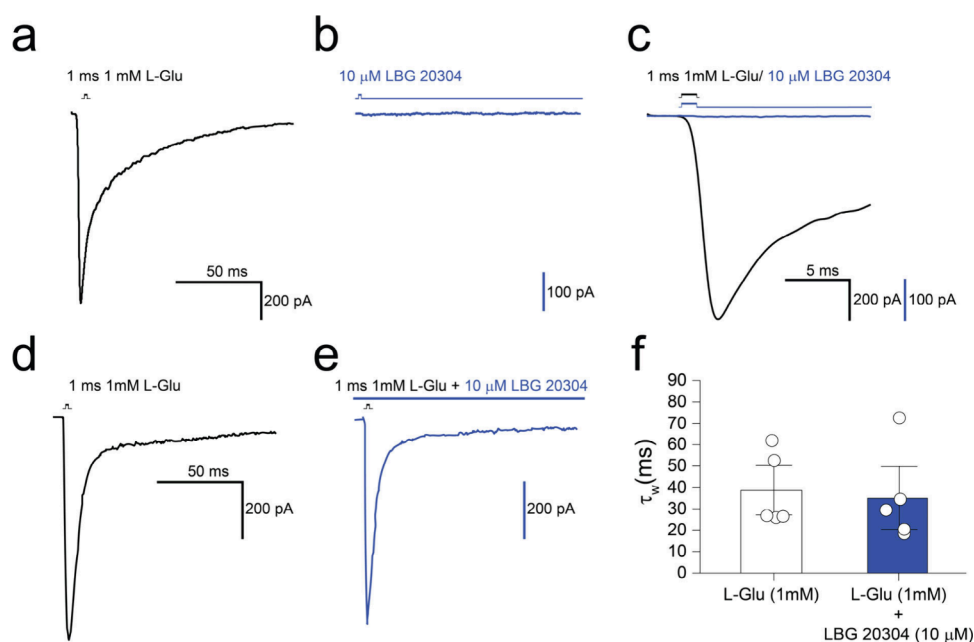


Figure 3. Testing agonist and/or antagonist activity of compound **LBG20304** on heteromeric GluK2/K5 receptors. (a–e) Example traces of heteromeric GluK2/K5. Example traces of (a) 1 ms application response to 1 mM L-Glu (in black) and (b) 1 ms application response to 10 μ M **LBG20304** (in blue). (c) Close-up trace from panels a and b. (d and e) Agonist evoked membrane currents in response to 1 ms application of 1 mM L-Glu (d, black) or 1 mM L-Glu in the presence of 10 μ M **LBG20304** (e, blue). (f) Summary bar graph of the deactivation kinetics of GluK2/K5 receptors in 1 mM L-Glu (white) or 1 mM L-Glu in the presence of 10 μ M **LBG20304**. There is no difference in the τ_w -weighted constant ($\tau_w = 38.7 \pm 7.7$ ms $n = 5$, for L-Glu (1 mM); $\tau_w = 35.1 \pm 22$ ms $n = 5$, for L-Glu (1 mM) + 2s 20304, p -value = 0.84).

occupying the primarily hydrophobic cavity lined by Leu60 and Ala139 (Figure 2A).

Functional Studies of Heteromeric GluK2/5 Receptors.

Equipped with the first selective GluK5 ligand **LBG20304**, we embarked on investigating its functional properties in heteromeric GluK2/K5 receptors expressed in HEK293T cells.²⁵ To do this, we compared responses to 1 mM Glu (1 ms) with responses to 10 μ M **LBG20304** in outside-out patch recordings (Figure 3a–c). The peak response to 1 mM Glu was large in amplitude and exhibited slow decay kinetics ($\tau = 3.52 \pm 0.3$ ms, $n = 11$) confirming that the response was due to the expression of heteromeric GluK2/K5 receptors, as noted previously (Figure 3a).^{2,26} In contrast, 10 μ M **LBG20304** alone failed to exhibit any measurable agonist response (Figure 3b). To determine whether **LBG20304** exhibited antagonist activity, we pretreated GluK2/K5 receptors with **LBG20304** prior to rapid application of 1 mM Glu (Figure 3d–f). In this case, the response to Glu alone was similar to the response observed following preincubation with **LBG20304** (normalized peak current = $100 \pm 3\%$, $n = 5$; data not shown; decay kinetics $\tau_w = 38.7 \pm 7.7$ ms $n = 5$, for L-Glu (1 mM); $\tau_w = 35.1 \pm 22$ ms $n = 5$, for L-Glu (1 mM) + **LBG20304**) suggesting that **LBG20304** does not exhibit any measurable antagonistic activity, at least at this concentration.

Functional Studies in Slices. We then proceeded to test the selective GluK5 ligand **LBG20304** on native neuronal kainate receptors in murine hippocampal neurons (Figure 4). To do so, we recorded from CA3 pyramidal cells in the mouse hippocampus, which are known to express functional heteromers containing GluK2 and GluK5 subunits.²⁷ Acute hippocampal slices were prepared from young adult wild-type mice, and CA3 pyramidal neurons were patch-clamped in the voltage clamp mode (holding potential -70 mV). The glutamatergic NMDA and AMPA receptors were blocked by a cocktail of

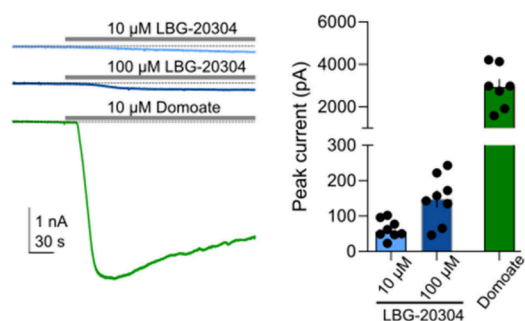


Figure 4. **LBG20304** is a weak agonist of native neuronal kainate receptors. Sample traces showing changes in holding current evoked by the bath application of **LBG20304** or domoate (left). Dot plot summarizing the results (right). Values are presented as mean \pm SEM.

selective antagonists (DAP-5 50 μ M and LY303070 20 μ M, respectively). After achieving a stable baseline for 3 to 5 min, we applied **LBG20304** (10 or 100 μ M) for 5 min. We observed a dose dependent change in the holding current, suggesting that **LBG20304** is a weak agonist of native heteromeric KA receptors containing GluK2/GluK5. In contrast, the bath application of the KA receptor agonist domoate (10 μ M) consistently elicited a larger change in the holding current (**LBG20304** 10 μ M = 56 ± 11 pA, $n = 9$ cells from 2 mice; **LBG20304** 100 μ M = 148 ± 24 pA, $n = 8$ cells from 2 mice; domoate 10 μ M = 2936 ± 377 , $n = 7$ cells from 2 mice).

CONCLUSION

In search for selective ligands for the GluK5 subunit, we have synthesized 21 analogues inspired by the natural product DA and characterized these in binding at homomeric GluK1-3,5 receptors. The analogue compound **LBG20304** displayed the highest affinity for GluK5 ($IC_{50} = 432$ nM) and >40-fold

selective over GluK1-3 and $\gg 100$ -fold selectivity over native AMPA and NMDA receptors. An MD simulation of LBG20304 gave insight into its interactions with the GluK5 orthosteric binding pocket. In an in vitro setup of heteromeric GluK2/5 receptors, LBG20304 at 10 μ M concentration did not activate the GluK2/5 receptor complex, nor did it antagonize these receptors after activation by Glu. Compound LBG20304 was further investigated in native murine receptors in hippocampal neurons known to express heteromeric KA receptors, where it is a dose-dependent manner (10 and 100 μ M) was a weak agonist.

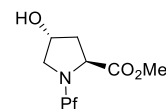
The fact that LBG20304 did not induce an agonist response at heteromeric GluK2/5 receptors is an interesting observation, which adds new details to discussions on requirements for KA receptor activation. The structural organization of the heteromeric GluK2/5 receptor as compared to homomeric GluK2 receptors have been investigated by cryoEM,² and it would highly interesting to determine the crystal structure of the GluK2/5 heteromeric receptor complex when binding of LBG20304.

EXPERIMENTAL SECTION

Chemistry. All reactions involving dry solvents or sensitive agents were performed under a nitrogen or argon atmosphere, and glassware was dried prior to use. Commercially available chemicals were used without further purification. Solvents were dried prior to use with an SG water solvent purification system or dried by standard methods. Reactions were monitored by analytical thin-layer chromatography (TLC, Merck silica gel 60 F254 aluminum sheets), analytical HPLC or UPLC-MS. Flash chromatography was carried out using the Merck silica gel 60 (15–40 μ m) or Merck silica gel 60 (40–63 μ m). ¹H NMR spectra were recorded on a 400 MHz Bruker Avance III or 600 MHz Bruker Avance III HD, and ¹³C NMR spectra on a 101 MHz Bruker Avance III or 151 MHz Bruker Avance III HD. Chemical shifts are reported in δ (ppm) relative to the singlet at $\delta = 7.26$ ppm of CDCl₃ and the singlet at 4.79 ppm of D₂O for ¹H NMR, and to the center line of the triplet at $\delta = 77.16$ ppm of CDCl₃ and the singlet at 67.19 ppm of 1,4-dioxane used as external reference in D₂O for ¹³C NMR. Analytical HPLC was performed using a Dionex HPLC system (Thermo Scientific) consisting of an LPG-3400A pump, a WPS-3000SL autosampler, and a DAD-3000D Diode Array Detector installed with a Phenomenex Gemini-NX 3 μ C18, 110 Å, 250 \times 4.60 mm column. Solvent A: H₂O + 0.1% TFA; Solvent B: MeCN-H₂O 9:1 + 0.1% TFA. For HPLC control, data collection and data handling, Chromeleon software v. 6.80 was used. Preparative HPLC was carried out on an Ultimate 3000 Thermo Scientific system with a HPG-3200BX pump, a Rheodyne 7725i injector, a 10 mL loop, an Ultimate MWD-3000SD detector (200, 210, 225, and 254 nm), and a Phenomenex Gemini-NX 5 μ C18 110 Å, 250 \times 21.20 mm column for preparative purifications or a Phenomenex Gemini-NX 5 μ C18 110 Å, 250 \times 10.00 mm column for semipreparative purifications. Solvent A: H₂O + 0.1% TFA; Solvent B: MeCN-H₂O 9:1 + 0.1% TFA. For HPLC control, data collection and data handling, Chromeleon software v. 6.80 was used.

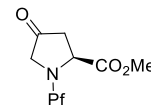
UPLC-MS spectra were recorded using an Acquity UPLC H-Class Waters series solvent delivery system equipped with an autoinjector coupled to an Acquity QDa and TUV detectors installed with a Acquity UPLCBECH C18 1.7 μ m column. Solvent A: 5% aq MeCN + 0.1% HCO₂H; Solvent B: MeCN + 0.1% HCO₂H. Usually, gradients from A:B 1:0 to 0:1 (5 min) or A:B 1:0 to 0–50 (5 min), were performed depending on the polarity of the compounds. For data collection and data handling, MassLynx software was used. Compounds were dried under high vacuum or freeze-dried using a ScanVac Cool Safe Freeze Drier. The purity of final compounds submitted for pharmacological characterization was determined by analytical HPLC to be >95%. Diastereomeric ratios were furthermore determined by ¹H NMR for selected compounds.

Methyl (2S,4R)-4-Hydroxy-1-(9-phenyl-9H-fluoren-9-yl)pyrrolidine-2-carboxylate (4).



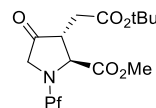
To a solution of commercially available methyl (2S,4R)-4-hydroxypyrrolidine-2-carboxylate hydrochloride (3, 10.0 g, 53.96 mmol) in anhydrous CH₂Cl₂ (200 mL), dried TEA (22.5 mL, 161.88 mmol) was added. The resulting white suspension was cooled to 0 °C and 9-bromo-9-phenyl-9H-fluorene (Pf-Br, 23.5 g, 70.15 mmol) was added in one portion, then, the starting suspension became a pale brown solution, and it was stirred at room temperature overnight. The reaction mixture was partitioned between CH₂Cl₂ (200 mL) and water (200 mL), then extractions with CH₂Cl₂ (3 \times 200 mL) were done. The collected organic layers were washed with brine (200 mL), dried over Na₂SO₄, filtered and the solvent of the filtrate was removed under reduced pressure to get a pale brown foam. This residue was purified by flash chromatography (heptane-EtOAc 7:3, isocratic) to afford pure product 4 (14.76 g, 71%) as a white solid. Characterization data obtained for alcohol 4 were identical to what is described in the literature.²¹ ¹H NMR (400 MHz, CDCl₃) δ 7.74 (d, *J* = 7.6 Hz, 1H), 7.65 (d, *J* = 7.5 Hz, 1H), 7.57–7.51 (m, 3H), 7.43 (td, *J* = 7.5, 1.0 Hz, 1H), 7.35–7.27 (m, 5H), 7.25–7.21 (m, 1H), 7.16 (td, *J* = 7.5, 1.0 Hz, 1H), 4.51 (dd, *J* = 11.1, 5.6 Hz, 1H), 3.58 (dd, *J* = 10.0, 5.3 Hz, 1H), 3.33–3.28 (m, 1H), 3.24 (s, 3H), 2.92 (dd, *J* = 10.1, 4.8 Hz, 1H), 2.03–1.96 (m, 1H), 1.84–1.76 (m, 1H).

Methyl (S)-4-Oxo-1-(9-phenyl-9H-fluoren-9-yl)pyrrolidine-2-carboxylate (5).



To a solution of alcohol 4 (7.4 g, 19.13 mmol) in anhydrous CH₂Cl₂ (200 mL), Dess-Martin periodinane (10.2 g, 22.95 mmol) was added and the resulting solution was stirred at room temperature overnight. The reaction mixture was quenched with 1 M aq Na₂S₂O₄ (200 mL) and extracted with CH₂Cl₂ (3 \times 200 mL). The collected organic layers were washed with 1 M aq NaHCO₃ (200 mL) and brine (200 mL), dried over Na₂SO₄, filtered and the solvent was removed under reduced pressure to give a white solid. This residue was purified by flash chromatography (heptane-EtOAc 9:1 to 85:15, gradient) to afford pure ketone 5 (5.3 g, 72%). Characterization data obtained for product 5 were identical with the described in the literature.²¹ ¹H NMR (400 MHz, CDCl₃) δ 7.75–7.69 (m, 2H), 7.50–7.43 (m, 3H), 7.43–7.36 (m, 3H), 7.32–7.26 (m, 3H), 7.26–7.21 (m, 2H), 3.82–3.72 (m, 2H), 3.48 (d, *J* = 17.9 Hz, 1H), 3.22 (s, 3H), 2.44 (dd, *J* = 18.0, 8.6 Hz, 1H), 2.29 (dd, *J* = 18.1, 2.8 Hz, 1H).

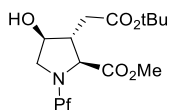
Methyl (2S,3R)-3-(2-(tert-Butoxy)-2-oxoethyl)-4-oxo-1-(9-phenyl-9H-fluoren-9-yl)pyrrolidine-2-carboxylate (6).



Ketone 5 (0.7 g, 1.83 mmol, 1 equiv) was loaded in a flame-dried flask with argon atmosphere and dissolved in 4.6 mL (0.4 M) anhydrous THF and 4.6 mL DMPU (0.4 M). The solution was

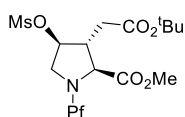
cooled to $-78\text{ }^{\circ}\text{C}$ and 0.77 mL nBuLi (2.5M, 1.92 mmol, 1.05 equiv) was added dropwise. The reaction mixture was stirred at $-78\text{ }^{\circ}\text{C}$ for 30 min after which *tert*-butyliodoacetate was added dropwise. After 10 min the reaction mixture was allowed to warm up to $-40\text{ }^{\circ}\text{C}$ and stirred at this temperature for 5 h. Saturated NH_4Cl was added, and the reaction was allowed to warm up to room temperature. Twenty mL water was added, and the aqueous layer was extracted with diethyl ether ($3 \times 50\text{ mL}$). The combined organic layers were dried over Na_2SO_4 , filtered and concentrated *in vacuo*. The residue was resuspended in 2 mL MeOH and left for crystallization at $-20\text{ }^{\circ}\text{C}$ overnight. The solid was filtered off and washed with cold MeOH (5 mL). The filtrate was concentrated again, and the process was repeated one more time. In total 0.543 g (58%) of the title compounds **6** was obtained as a single diastereomer.²¹ ^1H NMR (600 MHz, CDCl_3) δ 7.70 (dt, $J = 7.7, 1.4\text{ Hz}$, 2H), 7.52–7.48 (m, 3H), 7.43 (d, $J = 7.7\text{ Hz}$, 1H), 7.38 (tdd, $J = 7.6, 2.0, 1.1\text{ Hz}$, 2H), 3.82–3.75 (m, 1H), 3.45 (dd, $J = 11.9, 5.9\text{ Hz}$, 2H), 3.11 (s, 3H), 2.82 (ddd, $J = 7.7, 6.1, 4.8\text{ Hz}$, 1H), 2.47–2.34 (m, 2H), 1.31 (s, 9H). ^{13}C NMR (151 MHz, CDCl_3) δ : 211.9, 173.0, 169.7, 146.2, 144.6, 141.6, 141.2, 140.6, 129.0, 128.6, 128.1, 128.0, 127.8, 127.4, 127.1, 126.1, 120.3, 120.1, 81.5, 76.0, 63.9, 55.8, 51.6, 49.4, 34.4, 28.0.

Methyl (2S,3R,4S)-3-(2-(tert-Butoxy)-2-oxoethyl)-4-hydroxy-1-(9-phenyl-9H-fluoren-9-yl)pyrrolidine-2-carboxylate (7).



Ketone **6** (1.3 g, 2.6 mmol, 1 equiv) was dissolved in MeOH (52 mL, 0.05 M). To the suspension was added NaBH_4 (up to 2 equiv) in portions. The reaction was allowed to stir at rt for 3 h (completion by TLC). The reaction was quenched with NH_4Cl . Water (50 mL) was added, and the aqueous layer was extracted with EtOAc ($3 \times 50\text{ mL}$). The combined organic layers were dried over Na_2SO_4 , filtered and concentrated under reduced pressure. The crude material was purified by flash chromatography (heptane-EtOAc 4:1) to afford alcohol **7**, as a white foam (0.8 g, 59%, d.r. 7:1).²¹ ^1H NMR (600 MHz, chloroform-*d*) δ 7.78–7.76 (d, $J = 7.5\text{ Hz}$, 1H), 7.63 (dd, $J = 7.5, 1.1\text{ Hz}$, 1H), 7.58–7.53 (m, 2H), 7.49–7.44 (m, 2H), 7.36 (td, $J = 7.4, 1.1\text{ Hz}$, 1H), 7.30–7.22 (m, 5H), 7.12 (td, $J = 7.5, 1.1\text{ Hz}$, 1H), 4.43 (d, $J = 10.4\text{ Hz}$, 1H), 3.81 (ddt, $J = 10.4, 4.1, 2.1\text{ Hz}$, 1H), 3.43–3.39 (m, 1H), 3.30 (s, 3H), 3.18 (dd, $J = 10.3, 4.2\text{ Hz}$, 1H), 2.68 (d, $J = 2.8\text{ Hz}$, 1H), 2.34–2.28 (m, 1H), 1.88 (dd, $J = 15.5, 7.4\text{ Hz}$, 1H), 1.71 (dd, $J = 15.6, 8.4\text{ Hz}$, 1H), 1.32 (s, 9H). ^{13}C NMR (151 MHz, CDCl_3) δ 177.8, 170.6, 147.9, 145.3, 141.9, 141.8, 139.5, 129.0, 128.6, 128.6, 128.5, 128.5, 127.9, 127.6, 127.5, 127.5, 127.3, 127.0, 126.3, 120.4, 120.1, 81.2, 64.2, 55.3, 52.0, 48.4, 38.6, 28.0.

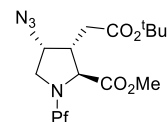
Methyl (2S,3R,4S)-3-(2-(tert-Butoxy)-2-oxoethyl)-4-((methylsulfonyl)oxy)-1-(9-phenyl-9H-fluoren-9-yl)pyrrolidine-2-carboxylate (8).



To a solution of alcohol **7** (1 g, 2.0 mmol, d.r. 7:1) in anhydrous CH_2Cl_2 (20 mL), dried TEA (530 μL , 2 equiv), was added. The resulting solution was cooled to $0\text{ }^{\circ}\text{C}$ and methanesulfonyl chloride (MsCl , 470 μL , 6 mmol, 3 equiv) was added. This

mixture was stirred at $0\text{ }^{\circ}\text{C}$ for 5 min and then at room temperature until full consumption of starting material (TLC control, 2h). The reaction mixture was partitioned between CH_2Cl_2 (30 mL) and water (30 mL) and then the aqueous layer was extracted with CH_2Cl_2 ($3 \times 30\text{ mL}$). The combined organic layers were washed with brine (30 mL), dried over Na_2SO_4 , filtered and the solvent was removed *in vacuo* to give a residue that was purified by flash chromatography (heptane-EtOAc 2:1, isocratic) to afford pure mesylate **8**, as a white foam (1.13 g, 75%, d.r. 7:1). ^1H NMR (400 MHz, CDCl_3) δ 7.74 (d, $J = 7.5\text{ Hz}$, 1H), 7.62 (d, $J = 7.5\text{ Hz}$, 1H), 7.53–7.50 (m, 2H), 7.48–7.42 (m, 2H), 7.38–7.27 (m, 5H), 7.25–7.20 (m, 1H), 7.14 (td, $J = 7.5, 1.0\text{ Hz}$, 1H), 4.67 (q, $J = 5.9\text{ Hz}$, 1H), 3.56 (d, $J = 6.1\text{ Hz}$, 2H), 3.26 (s, 3H), 3.04 (s, 3H), 2.76–2.68 (m, 2H), 2.17–2.03 (m, 2H), 1.32 (s, 9H). ^{13}C NMR (151 MHz, CDCl_3) δ 173.9, 169.9, 146.7, 145.9, 142.5, 141.8, 139.8, 129.2, 128.7, 128.7, 128.3, 127.7, 127.5, 127.4, 127.2, 127.2, 125.8, 120.4, 120.0, 81.4, 80.9, 76.4, 64.3, 53.8, 51.7, 45.9, 38.6, 36.7, 28.1. UPLC-MS (m/z) calcd for $\text{C}_{32}\text{H}_{35}\text{NO}_7\text{S}^+$ [$\text{M} + \text{H}$]⁺, 578.2; found, 578.2.

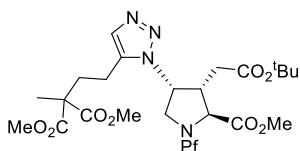
Methyl (2S,3R,4R)-4-Azido-3-(2-(tert-butoxy)-2-oxoethyl)-1-(9-phenyl-9H-fluoren-9-yl)pyrrolidine-2-carboxylate (9).



To a solution of mesylate **8** (1.13 g, 1.96 mmol, 1 equiv) sodium azide (1.27 g, 19.6 mmol, 10 equiv) in anhydrous DMPU (6.5 mL, 0.3 M) was added. The resulting solution was heated to $80\text{ }^{\circ}\text{C}$ and stirred at this temperature for 20 h. The reaction mixture was allowed to reach room temperature and it was partitioned between EtOAc (50 mL) and water (50 mL). The aqueous layer was extracted with EtOAc ($3 \times 50\text{ mL}$) and the combined layers were washed with brine (50 mL), dried over MgSO_4 , filtered and the solvent was removed under reduced pressure to give a pale yellow oil. This residue was purified by flash chromatography (heptane-EtOAc 5:1, isocratic) to afford pure azide **9**, as a white foam (0.9 g, 74%, d.r. 6:1). ^1H NMR (600 MHz, CDCl_3) δ 7.72 (dd, $J = 7.5, 1.1\text{ Hz}$, 1H), 7.61 (d, $J = 7.5\text{ Hz}$, 1H), 7.54 (m, 2H), 7.51 (d, $J = 7.6\text{ Hz}$, 1H), 7.46–7.41 (m, 1H), 7.35 (d, $J = 7.4\text{ Hz}$, 1H), 7.30–7.20 (m, 5H), 7.13 (t, $J = 7.5\text{ Hz}$, 1H), 4.37 (q, $J = 5.4\text{ Hz}$, 1H), 3.67 (dd, $J = 10.8, 5.5\text{ Hz}$, 1H), 3.21 (s, 3H), 3.12 (dd, $J = 10.8, 4.7\text{ Hz}$, 1H), 2.85 (d, $J = 6.2\text{ Hz}$, 1H), 2.61 (dq, $J = 8.9, 6.1\text{ Hz}$, 1H), 2.24 (dd, $J = 16.7, 8.8\text{ Hz}$, 1H), 1.83 (dd, $J = 16.7, 6.1\text{ Hz}$, 1H), 1.35 (s, 9H). ^{13}C NMR (151 MHz, CDCl_3) δ 175.1, 170.8, 147.1, 145.8, 142.4, 141.5, 139.9, 129.0, 128.6, 128.6, 127.7, 127.6, 127.5, 127.4, 127.2, 126.5, 120.1, 119.9, 80.9, 76.1, 64.9, 62.1, 53.3, 51.6, 43.9, 33.7, 28.1, 28.0. UPLC-MS (m/z) calcd for $\text{C}_{31}\text{H}_{33}\text{N}_4\text{O}_4^+$ [$\text{M} + \text{H}$]⁺, 525.2; found, 525.1.

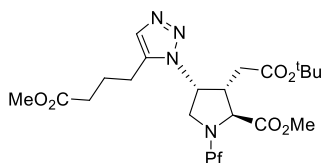
General Procedure A (synthesis of triazole intermediates 10a–j, l–u). A dried microwave vial with argon atmosphere was charged with **9** (50 mg, 0.01 mmol, 1 equiv) and $\text{Cp}^*\text{RuCl}(\text{PPh}_3)_2$ (6 mg, 10 mol %). The vial was evaporated and refilled with argon three times. Then anhydrous THF (1 mL, 0.1 M) was added, followed by the appropriate alkyne (2.5 equiv). The vial was capped and irradiated for 2 h at $100\text{ }^{\circ}\text{C}$ in a microwave oven. The reaction mixture was concentrated to dryness and purified by flash column chromatography on silica gel to give the desired product. For the majority of analogues, the product could be separated from its C'4-epimer, if not, the d.r. was determined by ^1H NMR.

Dimethyl 2-(2-(1-((3*R*,4*R*,5*S*)-4-(2-(*tert*-Butoxy)-2-oxoethyl)-5-(methoxycarbonyl)-1-(9-phenyl-9*H*-fluoren-9-yl)pyrrolidin-3-yl)-1*H*-1,2,3-triazol-5-yl)ethyl)-2-methylmalonate (**10a**).



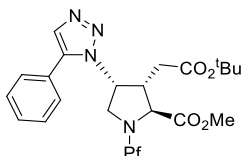
Dimethyl 2-(but-3-yn-1-yl)-2-methylmalonate was used as described in the general procedure A to afford **10b** after column chromatography: heptane-EtOAc 3:2, isocratic, as a white foam (78 mg, 77%). Mixture of conformers and C4 diastereomers, ratio could not be determined. ¹H NMR (600 MHz, CDCl₃) δ 7.73 (m, 2H), 7.66 (m, 3H), 7.51 (m, 1H), 7.47 (m, 1H), 7.44–7.40 (m, 2H), 7.37–7.32 (m, 1H), 7.28 (m, 2H), 7.25–7.21 (m, 2H), 5.25 (q, *J* = 7.7 Hz, 1H), 3.88 (m, 2H), 3.76 (m, 6H), 3.31 (bs, 1H), 3.26 (s, 3H), 2.97 (bs, 1H), 2.70–2.56 (m, 2H), 2.25–2.06 (m, 4H), 1.84 (d, *J* = 7.4 Hz, 3H), 1.18 (s, 9H). ¹³C NMR (151 MHz, CDCl₃) δ 172.2, 171.0, 170.1, 144.6, 141.3, 140.3, 137.8, 131.5, 129.4, 129.1, 128.7, 128.4, 128.0, 127.7, 127.6, 127.5, 127.0, 120.4, 120.2, 82.9, 80.9, 69.3, 65.5, 56.8, 56.5, 53.3, 53.0, 51.9, 51.6, 42.7, 42.6, 34.2, 33.8, 32.2, 31.5, 28.0, 27.9, 20.5, 18.9, 18.6.

Methyl (2*S*,3*R*,4*R*)-1-((9*H*-Fluoren-9-yl)(phenyl)methyl)-3-(2-(*tert*-butoxy)-2-oxoethyl)-4-(5-(4-methoxy-4-oxobutyl)-1*H*-1,2,3-triazol-1-yl)pyrrolidine-2-carboxylate (**10b**).



Carried out according to general procedure A and isolated by column chromatography (heptane-EtOAc 2:1, isocratic). White foam, (46 mg, 74%). ¹H NMR (600 MHz, CDCl₃) δ 7.75 (d, *J* = 7.4 Hz, 1H), 7.65 (t, *J* = 8.2 Hz, 2H), 7.59 (d, *J* = 7.5 Hz, 2H), 7.47 (td, *J* = 7.5, 1.2 Hz, 1H), 7.43–7.36 (m, 3H), 7.31 (m, 1H), 7.25–7.23 (m, 2H), 7.23–7.20 (m, 1H), 7.17 (t, *J* = 7.5 Hz, 1H), 5.20 (dt, *J* = 9.6, 6.9 Hz, 1H), 4.03 (t, *J* = 9.3 Hz, 1H), 3.78–3.74 (m, 1H), 3.26 (d, *J* = 1.2 Hz, 3H), 3.05 (d, *J* = 2.7 Hz, 1H), 2.74 (qd, *J* = 7.4, 2.6 Hz, 1H), 2.67 (t, *J* = 7.8 Hz, 2H), 2.41 (t, *J* = 7.2 Hz, 2H), 2.05–1.93 (m, 2H), 1.91–1.74 (m, 2H), 1.18 (s, 9H). ¹³C NMR (151 MHz, CDCl₃) δ 175.2, 173.2, 170.4, 147.1, 145.3, 141.7, 141.5, 140.0, 137.4, 132.0, 129.1, 128.8, 128.6, 128.2, 127.7, 127.5, 127.3, 127.2, 126.8, 120.3, 120.1, 80.8, 75.7, 65.1, 56.9, 51.9, 51.7, 50.2, 42.6, 34.4, 33.2, 27.9, 23.1, 22.6.

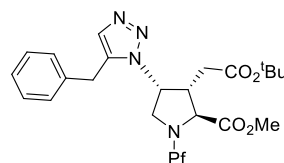
Methyl (2*S*,3*R*,4*R*)-1-((9*H*-Fluoren-9-yl)(phenyl)methyl)-3-(2-(*tert*-butoxy)-2-oxoethyl)-4-(5-phenyl-1*H*-1,2,3-triazol-1-yl)pyrrolidine-2-carboxylate (**10c**).



Carried out according to general procedure A and isolated by column chromatography (heptane-EtOAc 2:1, isocratic). **10c** was obtained as a light yellow foam (50 mg, 84%). ¹H NMR (600 MHz, CDCl₃) δ 7.77–7.71 (m, 1H), 7.65 (dd, *J* = 7.5, 3.7 Hz, 2H), 7.63 (s, 1H), 7.56–7.53 (m, 2H), 7.51–7.41 (m, 7H),

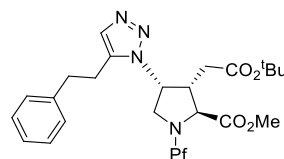
7.32 (d, *J* = 7.6 Hz, 1H), 7.29 (t, *J* = 7.5 Hz, 1H), 7.24 (m, 2H), 7.22–7.18 (m, 1H), 7.14 (t, *J* = 7.5 Hz, 1H), 5.33 (dt, *J* = 9.4, 7.0 Hz, 1H), 3.99 (t, *J* = 9.2 Hz, 1H), 3.69 (dd, *J* = 9.1, 6.7 Hz, 1H), 3.20 (s, 3H), 3.04 (d, *J* = 2.6 Hz, 1H), 2.71 (qd, *J* = 7.4, 2.6 Hz, 1H), 2.22 (dd, *J* = 17.0, 7.9 Hz, 1H), 1.94 (dd, *J* = 17.0, 7.0 Hz, 1H), 1.19 (s, 9H). ¹³C NMR (151 MHz, CDCl₃) δ 174.8, 170.5, 147.0, 145.4, 141.7, 141.5, 140.0, 139.1, 132.8, 129.8, 129.2, 129.2, 129.1, 128.7, 128.5, 128.2, 127.7, 127.5, 127.3, 127.1, 127.0, 126.8, 120.3, 120.1, 80.8, 75.7, 65.2, 57.3, 51.6, 50.9, 43.3, 35.0, 28.0.

Methyl (2*S*,3*R*,4*R*)-1-((9*H*-Fluoren-9-yl)(phenyl)methyl)-4-(5-benzyl-1*H*-1,2,3-triazol-1-yl)-3-(2-(*tert*-butoxy)-2-oxoethyl)pyrrolidine-2-carboxylate (**10d**).



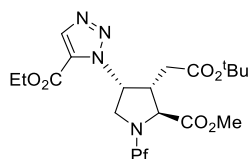
Carried out according to general procedure A and isolated by column chromatography (heptane-EtOAc 2:1, isocratic). **10d** was obtained as light yellow foam (53 mg, 87%). ¹H NMR (600 MHz, CDCl₃) δ 7.74 (d, *J* = 7.5 Hz, 1H), 7.63 (d, *J* = 7.7 Hz, 2H), 7.54 (d, *J* = 1.7 Hz, 1H), 7.47–7.44 (m, 1H), 7.40 (t, *J* = 7.5 Hz, 1H), 7.33 (d, *J* = 7.6 Hz, 1H), 7.31–7.27 (m, 4H), 7.24 (d, *J* = 7.7 Hz, 1H), 7.21 (d, *J* = 7.1 Hz, 1H), 7.17–7.13 (m, 3H), 5.17 (dt, *J* = 9.2, 6.9 Hz, 1H), 3.94 (t, *J* = 9.2 Hz, 1H), 3.25 (s, 3H), 3.01 (d, *J* = 2.5 Hz, 1H), 2.43 (qd, *J* = 7.4, 2.5 Hz, 1H), 1.79 (dd, *J* = 7.7, 1.6 Hz, 2H), 1.19 (s, 9H). ¹³C NMR (151 MHz, CDCl₃) δ 175.1, 170.3, 147.1, 145.3, 141.7, 141.5, 140.0, 137.2, 136.2, 133.4, 129.0, 129.0, 128.8, 128.7, 128.5, 128.2, 127.7, 127.5, 127.4, 127.3, 127.0, 126.7, 120.3, 120.0, 80.7, 75.6, 64.8, 57.1, 51.6, 50.0, 42.4, 34.4, 29.6, 28.0.

Methyl (2*S*,3*R*,4*R*)-1-((9*H*-Fluoren-9-yl)(phenyl)methyl)-3-(2-(*tert*-butoxy)-2-oxoethyl)-4-(5-phenethyl-1*H*-1,2,3-triazol-1-yl)pyrrolidine-2-carboxylate (**10e**).



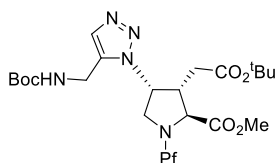
Carried out according to general procedure A and isolated by column chromatography (heptane-EtOAc 2:1, isocratic). **10e** was obtained as a light yellow foam (50 mg, 80%). ¹H NMR (600 MHz, CDCl₃) δ 7.74 (d, *J* = 7.5 Hz, 1H), 7.65–7.63 (m, 2H), 7.59–7.55 (m, 2H), 7.48–7.44 (m, 1H), 7.40 (t, *J* = 7.4 Hz, 1H), 7.38 (s, 1H), 7.36 (d, *J* = 7.9 Hz, 1H), 7.31–7.27 (m, 4H), 7.22 (m, 2H), 7.19–7.14 (m, 3H), 5.08 (dt, *J* = 9.3, 6.9 Hz, 1H), 3.93 (t, *J* = 9.3 Hz, 1H), 3.59 (dd, *J* = 9.3, 6.9 Hz, 1H), 3.25 (s, 3H), 3.04 (d, *J* = 2.7 Hz, 1H), 3.00–2.88 (m, 4H), 2.67 (dt, *J* = 7.4, 3.7 Hz, 1H), 1.78 (d, *J* = 7.4 Hz, 2H), 1.19 (s, 9H). ¹³C NMR (151 MHz, CDCl₃) δ 175.2, 170.4, 147.1, 145.3, 141.7, 141.5, 140.0, 139.9, 137.6, 132.2, 129.0, 128.8, 128.7, 128.6, 128.5, 128.2, 127.7, 127.5, 127.3, 127.1, 126.8, 126.8, 120.3, 120.1, 80.8, 75.7, 65.0, 56.8, 51.7, 50.2, 42.7, 34.6, 34.3, 28.0, 25.1.

Ethyl 1-((3*R*,4*R*,5*S*)-1-((9*H*-Fluoren-9-yl)(phenyl)methyl)-4-(2-(*tert*-butoxy)-2-oxoethyl)-5-(methoxycarbonyl)pyrrolidin-3-yl)-1*H*-1,2,3-triazol-5-carboxylate (**10f**).



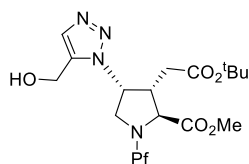
Carried out according to general procedure A and isolated by column chromatography (heptane-EtOAc 2:1, isocratic). Light brown foam (21 mg, 35% (d.r. 13:1). ^1H NMR (600 MHz, CDCl_3 , major isomer) δ 7.86 (s, 1H), 7.74 (d, $J = 8.0$ Hz, 1H), 7.67 (d, $J = 7.6$ Hz, 1H), 7.58 (m, 2H), 7.47–7.40 (m, 3H), 7.39–7.34 (m, 3H), 7.29–7.27 (m, 2H), 7.25–7.20 (m, 2H), 5.48 (q, $J = 7.4$ Hz, 1H), 4.40 (q, $J = 7.2$ Hz, 2H), 3.88 (dd, $J = 9.7$, 7.1 Hz, 1H), 3.64 (dd, $J = 9.7$, 7.8 Hz, 1H), 3.24 (s, 3H), 3.20 (d, $J = 3.7$ Hz, 1H), 2.98–2.92 (m, 1H), 1.79 (dd, $J = 16.7$, 8.1 Hz, 1H), 1.70–1.66 (m, 1H), 1.39 (t, $J = 7.2$ Hz, 3H), 1.23 (s, 9H). ^{13}C NMR (151 MHz, CDCl_3) δ 174.2, 169.7, 160.6, 146.0, 145.5, 141.3, 140.9, 140.2, 139.8, 129.0, 128.8, 128.7, 128.5, 128.1, 128.0, 127.7, 127.3, 127.3, 127.2, 126.7, 126.2, 120.3, 120.0, 81.2, 75.4, 64.6, 61.3, 60.1, 51.7, 50.6, 43.4, 33.7, 27.8, 27.8.

Methyl (2*S*,3*R*,4*R*)-1-((9*H*-Fluoren-9-yl)(phenyl)methyl)-3-(2-(*tert*-butoxy)-2-oxoethyl)-4-(5-(((*tert*-butoxycarbonyl)amino)methyl)-1*H*-1,2,3-triazol-1-yl)pyrrolidine-2-carboxylate (**10g**).



Carried out according to general procedure A and isolated by column chromatography (heptane-EtOAc 2:1, isocratic). Yellow foam (55 mg, 85%, d.r. 11:1). ^1H NMR (600 MHz, CDCl_3) δ 7.75 (d, $J = 7.5$ Hz, 1H), 7.65 (d, $J = 7.6$ Hz, 1H), 7.63 (d, $J = 7.7$ Hz, 1H), 7.58 (m, 2H), 7.50 (s, 1H), 7.47 (t, $J = 7.4$ Hz, 1H), 7.41 (t, $J = 7.5$ Hz, 1H), 7.38 (d, $J = 7.6$ Hz, 1H), 7.30 (t, $J = 7.5$ Hz, 1H), 7.25–7.23 (m, 2H), 7.18 (t, $J = 7.5$ Hz, 1H), 5.37 (s, 1H), 5.28 (q, $J = 7.8$, 6.6 Hz, 1H), 4.49 (d, $J = 15.6$ Hz, 1H), 4.29 (dd, $J = 15.6$, 5.0 Hz, 1H), 3.96 (s, 1H), 3.74 (dd, $J = 9.3$, 6.8 Hz, 1H), 3.26 (s, 3H), 3.03 (s, 1H), 2.80 (dq, $J = 9.0$, 4.6, 4.2 Hz, 1H), 2.20 (dd, $J = 17.6$, 9.5 Hz, 1H), 1.82 (d, $J = 18.0$ Hz, 1H), 1.44 (s, 9H), 1.17 (s, 9H). ^{13}C NMR (151 MHz, CDCl_3) δ 174.7, 170.7, 155.7, 146.8, 145.1, 141.7, 141.5, 140.0, 135.4, 133.1, 129.06, 128.8, 128.6, 128.2, 127.7, 127.5, 127.3, 126.8, 120.3, 120.0, 81.2, 75.7, 65.5, 57.2, 51.7, 50.6, 42.5, 34.7, 33.6, 29.9, 28.5, 28.0, 27.9.

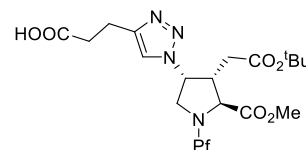
Methyl (2*S*,3*R*,4*R*)-1-((9*H*-Fluoren-9-yl)(phenyl)methyl)-3-(2-(*tert*-butoxy)-2-oxoethyl)-4-(5-(hydroxymethyl)-1*H*-1,2,3-triazol-1-yl)pyrrolidine-2-carboxylate (**10h**).



Carried out according to general procedure A and isolated by column chromatography (heptane-EtOAc 1:2, isocratic). White foam (36 mg, 65%). ^1H NMR (600 MHz, CDCl_3) δ 7.77 (d, $J = 7.4$ Hz, 1H), 7.66 (t, $J = 7.5$ Hz, 2H), 7.60 (d, $J = 7.5$ Hz, 2H),

7.52 (s, 1H), 7.49 (t, $J = 7.4$ Hz, 1H), 7.44 (d, $J = 7.4$ Hz, 1H), 7.37 (d, $J = 7.6$ Hz, 1H), 7.30 (t, $J = 7.5$ Hz, 1H), 7.29–7.26 (m, 2H), 7.24–7.20 (m, 1H), 7.17 (t, $J = 7.5$ Hz, 1H), 5.44 (dt, $J = 9.8$, 7.0 Hz, 1H), 4.80–4.69 (m, 2H), 4.08 (t, $J = 9.5$ Hz, 1H), 3.81–3.70 (m, 1H), 3.29 (s, 3H), 3.24 (t, $J = 5.5$ Hz, 1H), 2.94–2.86 (m, 2H), 2.34 (dd, $J = 18.0$, 10.4 Hz, 1H), 1.81 (dd, $J = 18.0$, 4.0 Hz, 1H), 1.15 (s, 9H). ^{13}C NMR (151 MHz, CDCl_3) δ 174.7, 171.4, 146.9, 144.9, 141.7, 141.6, 139.9, 136.8, 133.1, 129.1, 128.8, 128.6, 128.2, 127.6, 127.5, 127.3, 127.3, 126.9, 120.3, 120.1, 81.7, 75.7, 65.6, 57.6, 53.4, 51.8, 50.1, 42.2, 35.1, 28.0.

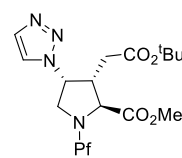
3-(1-((3*R*,4*R*,5*S*)-4-(2-(*tert*-Butoxy)-2-oxoethyl)-5-(methoxycarbonyl)-1-(9-phenyl-9*H*-fluoren-9-yl)pyrrolidin-3-yl)-1*H*-1,2,3-triazol-4-yl)propanoic Acid (**10j**).



A mixture of azide **9** (27 mg, 0.0515 mmol), 4-pentynoic acid (16 mg, 0.154 mmol) and copper(I) iodide (1.5 mg, 0.0079 mmol) in DMF-MeOH 9:1 (290 μL) was heated to 90 $^\circ\text{C}$ and stirred overnight under an Ar atmosphere. The reaction mixture was allowed to reach room temperature, it was partitioned between EtOAc (10 mL) and water (10 mL), and extractions with EtOAc (3 \times 10 mL) were done. The collected organic layers were washed with water (10 mL) and brine (10 mL), dried over MgSO_4 , filtered and the solvent was removed under reduced pressure to get a yellow oil. The residue was purified by flash chromatography (heptane-EtOAc 9:1 to 1:1 + CH_3COOH , gradient) to afford pure compound **10j** (19 mg, 59% (d.r. 12:1). ^1H NMR (600 MHz, CDCl_3) δ 7.75 (d, $J = 7.5$ Hz, 1H), 7.66 (d, $J = 7.5$ Hz, 1H), 7.61–7.57 (t, $J = 6.6$ Hz, 3H), 7.45 (t, $J = 7.5$ Hz, 1H), 7.41–7.35 (m, 2H), 7.33 (t, $J = 7.4$ Hz, 1H), 7.28 (t, $J = 7.2$ Hz, 2H), 7.24–7.18 (m, 2H), 7.15 (s, 1H), 5.38 (dd, $J = 15.0$, 7.4 Hz, 1H), 3.83 (dd, $J = 9.4$, 6.8 Hz, 1H), 3.67 (dd, $J = 12.2$, 5.9 Hz, 1H), 3.12 (d, $J = 3.3$ Hz, 1H), 2.97 (t, $J = 7.2$ Hz, 2H), 2.87–2.83 (m, 1H), 2.73 (t, $J = 7.2$ Hz, 2H), 1.73 (dd, $J = 16.4$, 8.6 Hz, 1H), 1.65 (dd, $J = 16.6$, 6.5 Hz, 1H), 1.23 (s, 9H). ^{13}C NMR (151 MHz, CDCl_3) δ 176.5, 174.8, 170.2, 146.6, 145.9, 145.6, 141.5, 141.3, 140.2, 129.1, 128.9, 128.6, 128.2, 127.8, 127.5, 126.5, 122.0, 120.4, 120.2, 81.1, 75.6, 64.7, 59.6, 51.8, 50.4, 43.6, 34.0, 33.4, 27.9, 20.8. UPLC-MS (m/z) calcd for $\text{C}_{36}\text{H}_{39}\text{N}_4\text{O}_6^+$ [$\text{M} + \text{H}$] $^+$, 623.3; found, 623.3.

4-Epimer: ^1H NMR (600 MHz, CDCl_3) δ 8.14 (s, 0.08H), 4.86 (q, $J = 6.3$ Hz, 0.08H), 4.12 (q, $J = 7.1$ Hz, 0.13H), 3.58 (br d, $J = 7.0$ Hz, 0.16H), 3.26 (s, 3H), 3.17 (s, 0.24H), 3.10 (t, $J = 7.2$ Hz, 0.14H), 3.05–3.00 (m, 0.14H), 2.90 (d, $J = 6.1$ Hz, 0.08H), 2.80 (t, $J = 7.5$ Hz, 0.16H), 2.70 (t, $J = 6.6$ Hz, 0.16H), 2.62 (t, $J = 6.4$ Hz, 0.16H), 1.26 (s, $J = 3.8$ Hz, 0.88H). ^{13}C NMR (151 MHz, CDCl_3) δ 175.9, 174.4, 172.9, 172.1, 171.3, 170.1, 169.7, 146.7, 145.8, 145.3, 142.2, 141.6, 141.5, 129.2, 128.7, 128.2, 127.9, 127.4, 127.2, 126.9, 126.0, 122.1, 120.5, 120.0, 81.6, 81.0, 76.2, 68.2, 65.4, 63.1, 60.6, 54.5, 52.1, 51.8, 51.7, 50.3, 47.3, 38.4, 33.7, 33.5, 33.3, 29.9, 28.0, 27.5, 22.8, 21.2, 21.0, 20.9, 20.7, 14.4.

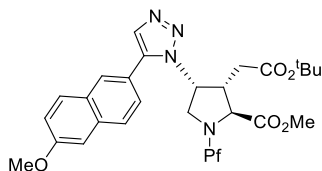
Methyl (2*S*,3*R*,4*R*)-3-(2-(*tert*-Butoxy)-2-oxoethyl)-1-(9-phenyl-9*H*-fluoren-9-yl)-4-(1*H*-1,2,3-triazol-1-yl)pyrrolidine-2-carboxylate (**10k**).



To a solution of azide **9** (53 mg, 0.101 mmol) and copper(I) iodide (2 mg, 0.0101 mmol) in DMF-MeOH 9:1 (560 μ L), ethynyltrimethylsilane (44 μ L, 0.303 mmol) was added and the resulting solution was heated to 90 °C and stirred at this temperature for 4 days. After this period, the reaction mixture was partitioned between EtOAc (10 mL) and water (10 mL), then, extractions with EtOAc (3 \times 10 mL) were done. The collected organic layers were washed with water (10 mL) and brine (10 mL), dried over MgSO₄, filtered and the solvent was removed under reduced pressure to get a pale brown oil (53 mg). This residue was redissolved in anhydrous THF (1.5 mL), 1 M TBAF in THF (222 μ L, 0.222 mmol) was added and the resulting mixture was stirred at room temperature overnight. The reaction mixture was quenched by adding water dropwise, then, it was partitioned between EtOAc (10 mL) and brine (10 mL). Extractions with EtOAc (3 \times 10 mL) were done and the collected organic layers were dried over MgSO₄, filtered and the solvent was removed under reduced pressure to afford a pale brown oil. Flash chromatography purification (silica gel, heptane-EtOAc 6:4, isocratic) provided the pure desired triazole **10k** (33 mg, 59%, d.r. 12:1) as a white solid. ¹H NMR (400 MHz, CDCl₃) δ 7.75 (d, *J* = 7.4 Hz, 1H), 7.67 (d, *J* = 7.4 Hz, 1H), 7.65–7.58 (m, *J* = 7.7, 5.6 Hz, 4H), 7.48–7.27 (m, 7H), 7.25–7.19 (m, 2H), 5.46 (dd, *J* = 15.4, 7.3 Hz, 1H), 3.87 (dd, *J* = 9.4, 7.0 Hz, 1H), 3.73 (t, *J* = 9.0 Hz, 1H), 3.27 (s, 3H), 3.18 (br d, *J* = 4.5 Hz, 1H), 2.96–2.85 (m, 1H), 1.76 (dd, *J* = 16.6, 8.3 Hz, 1H), 1.68 (dd, *J* = 16.8, 6.8 Hz, 1H), 1.23 (s, 9H). ¹³C NMR (151 MHz, CDCl₃) δ 174.3, 170.0, 146.2, 145.3, 141.2, 141.2, 140.3, 133.5, 129.2, 129.0, 128.6, 128.2, 127.9, 127.6, 127.5, 127.3, 126.6, 124.4, 120.4, 120.2, 81.1, 75.9, 64.9, 59.5, 51.8, 50.8, 43.6, 33.9, 28.0.

4-Epimer: ¹H NMR (400 MHz, CDCl₃) δ 8.39 (s, 0.08H), 4.95 (q, *J* = 6.0 Hz, 0.08H), 3.58 (d, *J* = 6.2 Hz, 0.16H), 2.25 (dd, *J* = 6.9, 2.0 Hz, 0.16H), 1.27 (s, *J* = 4.4 Hz, 1.73H). ¹³C NMR (151 MHz, CDCl₃) δ 174.2, 169.6, 145.8, 145.2, 142.1, 141.6, 134.2, 128.9, 128.7, 128.2, 127.9, 127.9, 126.9, 126.1, 122.7, 120.5, 120.1, 81.7, 76.2, 65.4, 62.9, 54.6, 51.8, 47.4, 38.5, 29.9.

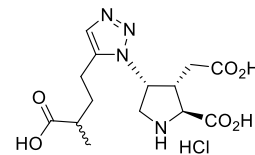
Methyl (2*S*,3*R*,4*R*)-1-((9*H*-Fluoren-9-yl)(phenyl)methyl)-3-(2-(*tert*-butoxy)-2-oxoethyl)-4-(5-(6-methoxynaphthalen-2-yl))-1*H*-1,2,3-triazol-1-yl)pyrrolidine-2-carboxylate (**10s**).



Carried out according to general procedure A and isolated by column chromatography: heptane-EtOAc 2:1, isocratic. **10s** was obtained as a light yellow foam (56 mg, 83%). ¹H NMR (600 MHz, CDCl₃) δ 7.86–7.82 (m, 2H), 7.78 (d, *J* = 8.8 Hz, 1H), 7.75 (d, *J* = 7.4 Hz, 1H), 7.70 (s, 1H), 7.65 (t, *J* = 8.2 Hz, 2H), 7.56–7.51 (m, 2H), 7.50–7.45 (m, 2H), 7.42 (t, *J* = 7.4 Hz, 1H), 7.32–7.27 (m, 2H), 7.23 (m, 3H), 7.20–7.17 (m, 2H), 7.13 (t, *J* = 7.5 Hz, 1H), 5.43 (dt, *J* = 9.3, 6.9 Hz, 1H), 3.99 (t, *J* = 9.3 Hz, 1H), 3.96 (s, 3H), 3.69 (dd, *J* = 9.1, 6.7 Hz, 1H), 3.18 (s, 3H), 3.06 (d, *J* = 2.6 Hz, 1H), 2.92 (s, 1H), 2.79 (qd, *J* = 7.4, 2.5 Hz, 1H), 2.26 (dd, *J* = 17.1, 7.9 Hz, 1H), 1.96 (dd, *J* = 17.0, 7.1 Hz, 1H), 1.19 (s, 9H). ¹³C NMR (151 MHz, CDCl₃) δ 174.8, 170.5, 158.9, 147.0, 145.3, 141.7, 141.5, 140.0, 139.3, 135.0, 132.9, 129.9, 129.1, 128.8, 128.7, 128.6, 128.5, 128.2, 127.9, 127.7, 127.5, 127.3, 127.1, 126.8, 126.6, 121.8, 120.23, 120.1, 105.9, 80.8, 75.7, 65.2, 57.3, 55.6, 51.6, 50.9, 43.4, 35.0, 28.0.

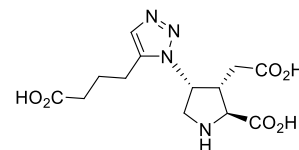
General Procedure B (global deprotection of 1,4-triazole and 1,5-triazole analogues). The appropriate triazole **10a–u** was refluxed in 6 M HCl (10 mL) overnight. The reaction mixture was condensed under reduced pressure to afford a crude yellow oil, which was redissolved in water (800 μ L) and purified by preparative HPLC. The resulting TFA salt was converted to its HCl salt by dissolving and evaporating from 1 M aq HCl (3 \times 2 mL).

(2*S*,3*R*,4*R*)-4-(5-(3-Carboxybutyl)-1*H*-1,2,3-triazol-1-yl)-3-(carboxymethyl)pyrrolidine-2-carboxylic Acid Hydrochloride (**2a**).



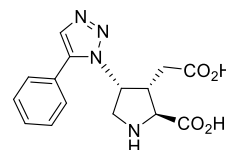
Carried out according to general procedure B. The product was isolated by preparative HPLC, Rt: 7.69 min; flow: 20 mL min⁻¹; gradient 0–50% B (25 min); λ = 210 nm. The salt was treated with 1 M aq HCl (2 mL) and the volatiles were evaporated under reduced pressure, repeating the same procedure three times to afford the desired hydrochloride salt as a white solid (15 mg, 36%, C4 d.r. > 99:1, C5' d.r. 1:1). ¹H NMR (600 MHz, D₂O) δ 7.73 (s, 1H), 5.65–5.58 (m, 1H), 4.64 (dd, *J* = 11.3, 2.2 Hz, 1H), 4.13 (ddd, *J* = 13.4, 6.2, 2.6 Hz, 1H), 3.90 (d, *J* = 13.2, 1H), 3.48–3.39 (m, 1H), 2.95 (m, 1H), 2.80–2.66 (m, 2H), 2.60 (m, 1H), 2.04–1.77 (m, 3H), 1.22 (m, 3H). ¹³C NMR (151 MHz, D₂O) δ 180.9, 174.2, 170.9, 139.7, 139.6, 132.2, 132.1, 62.8, 58.1, 50.8, 43.3, 38.8, 38.6, 31.3, 31.2, 31.0, 20.0, 19.9, 16.4. UPLC-MS (*m/z*) calcd for C₁₄H₂₀N₄O₆⁺ [M + H]⁺, 341.1; found, 341.5.

(2*S*,3*R*,4*R*)-3-(Carboxymethyl)-4-(5-(3-carboxypropyl)-1*H*-1,2,3-triazol-1-yl)pyrrolidine-2-carboxylic Acid (**2b**).



Carried out according to general procedure B, starting from **10b**. The product was isolated by preparative HPLC: Rt: 5.67 min; flow: 20 mL min⁻¹; gradient 0–50% B (25 min); λ = 210 nm. **2b** was obtained as a light yellow solid (10.0 mg, 40%, 3% of the C4 epimer). ¹H NMR (600 MHz, D₂O) δ 7.89 (s, 1H), 5.76 (t, *J* = 6.1 Hz, 1H), 4.63 (d, *J* = 11.1 Hz, 1H), 4.26 (dd, *J* = 13.3, 6.2 Hz, 1H), 4.04 (d, *J* = 13.4 Hz, 1H), 3.52 (tdd, *J* = 10.6, 6.0, 4.1 Hz, 1H), 3.10 (dd, *J* = 17.9, 4.1 Hz, 1H), 2.91 (t, *J* = 7.7 Hz, 2H), 2.65 (t, *J* = 7.2 Hz, 2H), 2.20–2.03 (m, 3H). ¹³C NMR (151 MHz, D₂O) δ 177.7, 174.3, 171.8, 139.5, 132.2, 63.6, 58.1, 50.7, 43.6, 32.7, 31.7, 22.6, 21.3. UPLC-MS (*m/z*) calcd for C₁₃H₁₈N₄O₆⁺ [M + H]⁺, 327.1; found, 327.5.

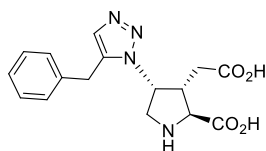
(2*S*,3*R*,4*R*)-3-(Carboxymethyl)-4-(5-phenyl-1*H*-1,2,3-triazol-1-yl)pyrrolidine-2-carboxylic Acid (**2c**).



Carried out according to general procedure B, starting from **10c**. The product was isolated by preparative HPLC: Rt: 10.2 min; flow: 20 mL min⁻¹; gradient 0–50% B (25 min); λ = 210 nm. **2c** was obtained as a light yellow solid (17.7 mg, 58%, d.r. > 99:1). ¹H NMR (600 MHz, D₂O) δ 7.96 (s, 1H), 7.65–7.57 (m, 3H),

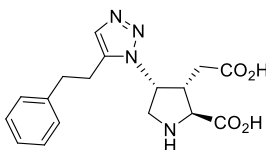
7.52–7.44 (m, 2H), 5.73 (dt, $J = 6.5, 3.7$ Hz, 1H), 4.52 (m, 1H), 4.18 (m, 2H), 3.21 (m, 1H), 2.88 (dd, $J = 18.1, 3.8$ Hz, 1H), 1.78 (dd, $J = 18.1, 10.7$ Hz, 1H). ^{13}C NMR (151 MHz, D_2O) δ 173.4, 171.3, 140.4, 133.0, 130.3, 129.3, 129.2, 129.2, 124.9, 62.9, 58.8, 50.6, 43.7, 31.1. UPLC-MS (m/z) calcd for $\text{C}_{15}\text{H}_{16}\text{N}_4\text{O}_4^+$ [$\text{M} + \text{H}$] $^+$, 317.1; found, 317.5.

(2*S*,3*R*,4*R*)-4-(5-Benzyl-1*H*-1,2,3-triazol-1-yl)-3-(carboxymethyl)pyrrolidine-2-carboxylic Acid (**2d**).



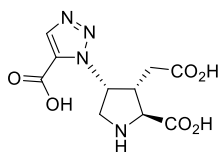
Carried out according to general procedure B, starting from **10d** and product isolated by preparative HPLC: Rt: 11.6 min; flow: 20 mL min^{-1} ; gradient 0–50% B (25 min); $\lambda = 210$ nm. The product **2d** was obtained as a white solid (15.5 mg, 51%, C4 epimer <1%). ^1H NMR (600 MHz, D_2O , performed with water suppression) δ 7.63 (s, 1H), 7.45–7.41 (m, 2H), 7.40–7.35 (m, 1H), 7.30–7.26 (m, 2H), 5.53 (t, $J = 6.2$ Hz, 1H), 4.54–4.49 (m, 1H), 4.21–4.18 (m, 1H), 4.08–4.05 (m, 1H), 3.93 (ddd, $J = 13.3, 6.3, 2.3$ Hz, 1H), 3.70 (d, $J = 13.4$ Hz, 1H), 3.30 (m, 1H), 2.87 (dd, $J = 17.9, 4.5$ Hz, 1H), 1.93 (dd, $J = 17.9, 10.0$ Hz, 1H). ^{13}C NMR (151 MHz, D_2O) δ 174.3, 171.7, 139.2, 136.2, 133.3, 129.2, 128.7, 127.4, 63.6, 58.5, 50.5, 43.3, 43.3, 31.6, 28.2. UPLC-MS (m/z) calcd for $\text{C}_{16}\text{H}_{18}\text{N}_4\text{O}_4^+$ [$\text{M} + \text{H}$] $^+$, 331.1; found, 331.5.

(2*S*,3*R*,4*R*)-3-(Carboxymethyl)-4-(5-phenethyl-1*H*-1,2,3-triazol-1-yl)pyrrolidine-2-carboxylic Acid (**2e**).



Carried out according to general procedure B, starting from **10e** and product isolated by preparative HPLC: Rt: 12.8 min; flow: 20 mL min^{-1} ; gradient 0–50% B (25 min); $\lambda = 210$ nm. **2e** was obtained as a white solid (11 mg, 38%, C4 epimer <1%). ^1H NMR (600 MHz, D_2O) δ 7.72 (s, 1H), 7.37 (m, 2H), 7.34–7.29 (m, 1H), 7.21–7.15 (m, 2H), 5.15 (t, $J = 6.4$ Hz, 1H), 4.29–4.24 (m, 1H), 3.67 (ddd, $J = 13.6, 6.4, 1.7$ Hz, 1H), 3.24–3.09 (m, 4H), 3.00–2.86 (m, 2H), 2.83 (dd, $J = 17.8, 4.2$ Hz, 1H), 1.71 (ddd, $J = 18.0, 10.6, 2.7$ Hz, 1H). ^{13}C NMR (151 MHz, D_2O) δ 174.5, 172.2, 140.0, 139.6, 132.7, 128.8, 128.8, 126.8, 63.7, 58.3, 50.1, 43.7, 34.4, 31.8, 23.8. UPLC-MS (m/z) calcd for $\text{C}_{17}\text{H}_{20}\text{N}_4\text{O}_4^+$ [$\text{M} + \text{H}$] $^+$, 345.2; found, 345.5.

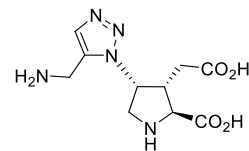
1-((3*R*,4*R*,5*S*)-5-Carboxy-4-(carboxymethyl)pyrrolidin-3-yl)-1*H*-1,2,3-triazole-5-carboxylic Acid (**2f**).



Carried out according to general procedure B, starting from **10f** and product isolated by preparative HPLC: Rt: 5.79 min; flow: 10 mL min^{-1} ; isocratic 100% A (25 min); $\lambda = 210$ nm. **2f** was obtained as a white solid (1.48 mg, 14%, C4 epimer <1%) (contains 10% of *tert*-butylated product). ^1H NMR (600 MHz, D_2O) δ 8.32 (s, 1H), 5.71 (t, $J = 6.1$ Hz, 1H), 4.19 (d, $J = 11.3$

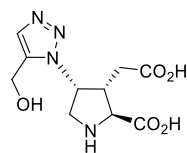
Hz, 1H), 4.08–4.04 (m, 1H), 3.96 (d, $J = 13.6$ Hz, 1H), 3.20 (m, 1H), 2.87–2.80 (m, 1H), 1.88–1.76 (m, 1H). ^{13}C NMR (151 MHz, D_2O) δ 174.5, 172.0, 165.3, 149.0, 129.6, 63.7, 62.1, 50.0, 43.6, 31.8. UPLC-MS (m/z) calcd for $\text{C}_{10}\text{H}_{12}\text{N}_4\text{O}_5^+$ [$\text{M} + \text{H}$] $^+$, 285.1; found, 285.5.

(2*S*,3*R*,4*R*)-4-(5-(Aminomethyl)-1*H*-1,2,3-triazol-1-yl)-3-(carboxymethyl)pyrrolidine-2-carboxylic Acid (**2g**).



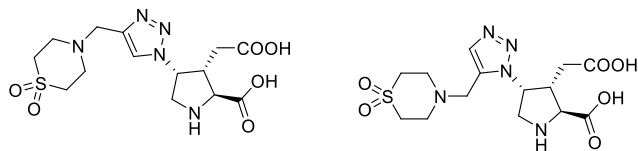
Carried out according to general procedure B, starting from **10g** and product isolated by preparative HPLC: Rt: 6.68 min; flow: 10 mL min^{-1} ; isocratic 100% A (25 min); $\lambda = 210$ nm. **2g** was isolated as a yellow solid (13.4 mg, 50%, C4 epimer <1%). ^1H NMR (600 MHz, D_2O) δ 7.93 (s, 1H), 5.74–5.66 (m, 1H), 4.38 (d, $J = 11.1$ Hz, 1H), 4.35 (m, 2H), 4.08–4.05 (m, 1H), 3.86 (dd, $J = 13.4, 1.4$ Hz, 1H), 3.31–3.25 (m, 1H), 2.90 (dd, $J = 17.8, 3.9$ Hz, 1H), 1.84 (dd, $J = 17.8, 11.0$ Hz, 1H). ^{13}C NMR (151 MHz, D_2O) δ 174.7, 171.6, 134.0, 132.2, 63.6, 59.2, 50.8, 43.6, 31.7, 31.4. UPLC-MS (m/z) calcd for $\text{C}_{10}\text{H}_{12}\text{N}_5\text{O}_4^+$ [$\text{M} + \text{H}$] $^+$, 270.1; found, 270.5.

(2*S*,3*R*,4*R*)-3-(Carboxymethyl)-4-(5-(hydroxymethyl)-1*H*-1,2,3-triazol-1-yl)pyrrolidine-2-carboxylic Acid (**2h**).



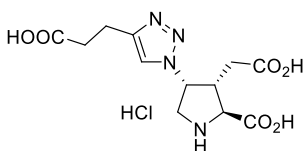
Carried out according to general procedure B, starting from **10h**. The product was isolated by preparative HPLC: Rt: 7.27 min; flow: 10 mL min^{-1} ; isocratic 100% A (25 min); $\lambda = 210$ nm. **2h** was obtained as a white solid (8.6 mg, 52%, C4 epimer <1%). ^1H NMR (600 MHz, D_2O) δ 7.76 (s, 1H), 5.64 (t, $J = 6.1$ Hz, 1H), 4.67 (t, $J = 14.4$ Hz, 2H), 4.60 (d, $J = 11.4$ Hz, 1H), 4.06 (dd, $J = 13.4, 6.1$ Hz, 1H), 3.82 (d, $J = 13.5$ Hz, 1H), 3.39 (m, 1H), 2.81 (dd, $J = 17.9, 4.5$ Hz, 1H), 1.99 (dd, $J = 17.8, 9.8$ Hz, 1H). ^{13}C NMR (151 MHz, D_2O) δ 174.3, 170.8, 138.5, 133.0, 63.0, 58.9, 51.6, 51.0, 43.2, 31.3. UPLC-MS (m/z) calcd for $\text{C}_{10}\text{H}_{14}\text{N}_4\text{O}_5^+$ [$\text{M} + \text{H}$] $^+$, 271.1; found, 271.5.

(2*S*,3*R*,4*R*)-3-(Carboxymethyl)-4-(5-((1,1-dioxidothiomorpholino)methyl)-1*H*-1,2,3-triazol-1-yl)pyrrolidine-2-carboxylic Acid (**2i**).



Prepared according to general procedure A and B. **2i** was obtained as a 1:2 mixture of it 4'-regioisomer. White solid, yield 6%. (4-phenyl-triazol:5-phenyl-triazol = 2:1) ^1H NMR (400 MHz, MeOD): δ 7.69 (s, 1H), 5.81 (t, $J = 6.2$ Hz, 1H), 4.61 (d, $J = 11.5$ Hz, 1H), 4.01–3.95 (m, 1H), 3.76 (m, 2H), 3.70 (m, 1H), 3.30 (m, 1H), 3.06–3.01 (m, 4H), 2.91 (m, 4H), 2.78 (dd, $J = 6.5, 4.7$ Hz, 1H), 1.85 (dd, $J = 18.0, 10.4$ Hz, 1H). ^{13}C NMR (101 MHz, MeOD) δ 172.54, 135.62, 133.87, 58.90, 50.88, 43.22, 30.64. UPLC-MS (m/z) calcd for $\text{C}_{14}\text{H}_{21}\text{N}_5\text{O}_4\text{S}^+$ [$\text{M} + \text{H}$] $^+$ 388.1, found 388.4.

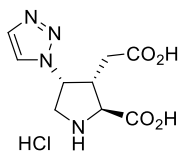
(2*S*,3*R*,4*R*)-4-(4-(2-Carboxyethyl)-1*H*-1,2,3-triazol-1-yl)-3-(carboxymethyl)pyrrolidine-2-carboxylic Acid Hydrochloride (**2j**).



Prepared according to general procedure B, starting from **10j**. HPLC Rt: 5.32 min; flow: 3 mL min⁻¹; isocratic 100% A (25 min); λ = 210 nm). The product **2j** was obtained as a white solid (5 mg, 56%, contains 8% of the C4-epimer). ¹H NMR (600 MHz, D₂O) δ 7.84 (s, 1H), 5.73 (t, *J* = 5.9 Hz, 1H), 4.47 (d, *J* = 11.5 Hz, 1H), 4.13 (dd, *J* = 13.6, 6.3 Hz, 1H), 4.04 (dd, *J* = 13.6, 1.4 Hz, 1H), 3.40–3.32 (m, 1H), 3.06 (t, *J* = 7.1 Hz, 2H), 2.89 (dd, *J* = 17.9, 4.3 Hz, 1H), 2.80 (t, *J* = 7.1 Hz, 2H), 1.80 (dd, *J* = 17.9, 10.3 Hz, 1H). ¹³C NMR (151 MHz, D₂O) δ 177.6, 174.8, 171.3, 147.1, 125.5, 67.2 (1,4-dioxane), 63.2, 61.9, 50.8, 43.9, 33.6, 31.9, 20.6. UPLC-MS (*m/z*) calcd for C₁₂H₁₇N₄O₆⁺ [M-Cl]⁺, 313.1; found, 313.0.

4-Epimer: ¹H NMR (600 MHz, D₂O) δ 7.98 (s, 0.08H), 5.42 (dd, *J* = 13.8, 6.6 Hz, 0.08H), 4.43 (d, *J* = 9.0 Hz, 0.16H), 4.09 (dd, *J* = 13.1, 8.0 Hz, 0.16H), 4.00 (dd, *J* = 13.1, 5.8 Hz, 0.16H), 3.01 (dd, *J* = 17.5, 5.2 Hz, 0.16H), 1.36 (dd, *J* = 6.6, 2.4 Hz, 0.07H). ¹³C NMR (151 MHz, D₂O) δ 177.7, 174.8, 147.5, 123.8, 67.2 (1,4-dioxane), 63.0, 49.2, 45.2, 35.2, 33.6, 20.6.

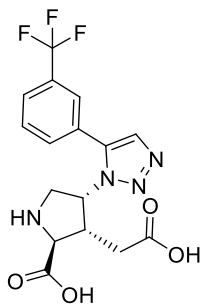
(2*S*,3*R*,4*R*)-3-(Carboxymethyl)-4-(1*H*-1,2,3-triazol-1-yl)pyrrolidine-2-carboxylic Acid Hydrochloride (**2k**).



Prepared according to general procedure B, starting from **10k**. HPLC Rt: 5.65 min; flow: 3 mL min⁻¹; isocratic 100% A (25 min); λ = 210 nm). White solid (8 mg, 47%, contains 4–5% of the C4-epimer). ¹H NMR (600 MHz, D₂O) δ 8.04 (d, *J* = 1.1 Hz, 1H), 7.89 (d, *J* = 0.9 Hz, 1H), 5.82 (t, *J* = 6.1 Hz, 1H), 4.61 (d, *J* = 11.6 Hz, 1H), 4.16 (dd, *J* = 13.8, 6.5 Hz, 1H), 4.04 (dd, *J* = 13.6, 1.7 Hz, 1H), 3.47–3.40 (m, 1H), 2.90–2.83 (m, 1H), 1.87 (ddd, *J* = 17.8, 10.0, 2.1 Hz, 1H). ¹³C NMR (151 MHz, D₂O) δ 174.8, 170.7, 134.2, 128.0, 62.8, 61.9, 51.1, 43.7, 31.7. UPLC-MS (*m/z*) calcd for C₉H₁₃N₄O₄⁺ [M-Cl]⁺, 241.0; found, 241.0.

C4-epimer: ¹H NMR (600 MHz, D₂O) δ 8.17 (s, 0.04H), 5.55–5.50 (m, 0.04H), 4.55 (d, *J* = 9.0 Hz, 0.05H), 4.13–4.10 (m, 0.05H), 3.05–3.00 (m, 0.05H), 2.93 (d, *J* = 7.9 Hz, 0.03H). ¹³C NMR (151 MHz, D₂O) δ 63.0, 49.5, 45.0, 35.1.

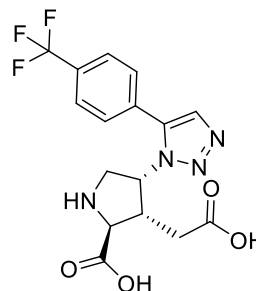
(2*S*,3*R*,4*R*)-3-(Carboxymethyl)-4-(5-(3-(trifluoromethyl)phenyl)-1*H*-1,2,3-triazol-1-yl)pyrrolidine-2-carboxylic Acid (**2l**).



Prepared according to general procedure A and B. The product was isolated by preparative HPLC: Rt: 9.8 min; flow: 20 mL

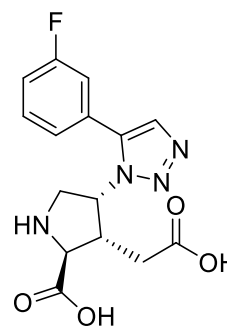
min⁻¹; gradient 0–50% B (25 min); λ = 210 nm. The product was obtained as a white solid in 20% yield over two steps, C4 epimer <1%. ¹H NMR (400 MHz, MeOD) δ 7.88 (s, 1H), 7.75 (d, *J* = 2.7 Hz, 2H), 7.68–7.63 (m, 2H), 5.57–5.49 (m, 1H), 4.52 (d, *J* = 11.6 Hz, 1H), 4.01 (dd, *J* = 13.2, 6.1 Hz, 1H), 3.92 (dd, *J* = 13.2, 1.5 Hz, 1H), 3.14 (m, 1H), 2.78 (dd, *J* = 18.0, 3.5 Hz, 1H), 1.71 (dd, *J* = 18.0, 11.0 Hz, 1H). ¹³C NMR (101 MHz, MeOD): δ 171.7, 168.9, 138.8, 133.31, 132.8, 129.9, 126.7, 126.5, 126.4, 125.8, 125.8, 62.4, 58.9, 50.7, 43.6, 30.5. UPLC-MS (*m/z*) calcd for C₁₆H₁₅F₃N₄O₄⁺ [M + H]⁺ 385.1, found 385.2.

(2*S*,3*R*,4*R*)-3-(Carboxymethyl)-4-(5-(4-(trifluoromethyl)phenyl)-1*H*-1,2,3-triazol-1-yl)pyrrolidine-2-carboxylic Acid (**2m**).



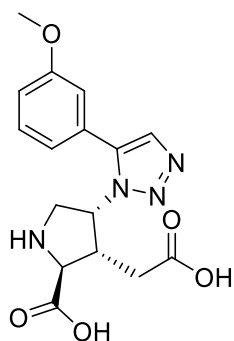
Prepared according to general procedure A and B. The product was isolated by preparative HPLC: Rt: 9.7 min; flow: 20 mL min⁻¹; gradient 0–50% B (25 min); λ = 210 nm. The product **2m** was obtained as a white solid in 27% yield over two steps, C4 epimer <1%. ¹H NMR (400 MHz, MeOD) δ 8.01 (s, 1H), 7.88 (t, *J* = 7.3 Hz, 2H), 7.73 (d, *J* = 8.0 Hz, 2H), 5.69 (t, *J* = 6.2 Hz, 1H), 4.74 (dd, *J* = 11.4, 6.4 Hz, 1H), 4.18 (m, 1H), 4.08 (m, 1H), 3.28 (m, 1H), 2.88 (m, 1H), 1.75 (dd, *J* = 17.9, 10.8 Hz, 1H). ¹³C NMR (101 MHz, MeOD): δ 171.6, 168.5, 139.1, 133.3, 129.8, 125.8, 62.2, 58.8, 50.9, 43.5, 30.4. UPLC-MS (*m/z*) calcd for C₁₆H₁₅F₃N₄O₄⁺ [M + H]⁺ 385.1, found 385.4.

(2*S*,3*R*,4*R*)-3-(Carboxymethyl)-4-(5-(3-fluorophenyl)-1*H*-1,2,3-triazol-1-yl)pyrrolidine-2-carboxylic Acid (**2n**).



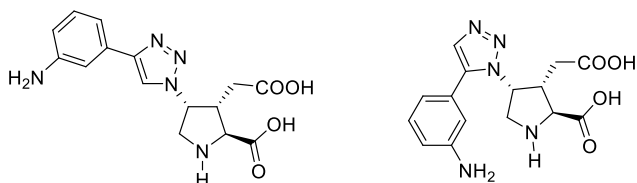
Prepared according to general procedure A and B. The product was isolated by preparative HPLC: Rt: 9.9 min; flow: 20 mL min⁻¹; gradient 0–50% B (25 min); λ = 210 nm. The product **2n** was obtained as a white solid in 46% yield over two steps, C4 epimer <1%. ¹H NMR (600 MHz, D₂O): δ 7.90 (s, 1H), 7.51 (q, *J* = 7.3 Hz, 1H), 7.35–7.15 (m, 3H), 5.62 (d, *J* = 6.5 Hz, 1H), 4.23 (d, *J* = 11.4 Hz, 1H), 4.11–4.01 (m, 2H), 3.02 (m, 1H), 2.76 (dd, *J* = 18.0, 3.6 Hz, 1H), 1.63 (dd, *J* = 18.0, 10.9 Hz, 1H) ppm. ¹³C NMR (151 MHz, D₂O): δ 163.32, 161.69, 131.33, 131.27, 125.39, 117.27, 117.13, 116.39, 116.23, 59.43, 50.66, 44.60 ppm. UPLC-MS (*m/z*) calcd for C₁₅H₁₅FN₄O₄⁺ [M + H]⁺ 335.1, found 335.2.

(2*S*,3*R*,4*R*)-3-(Carboxymethyl)-4-(5-(3-methoxyphenyl)-1*H*-1,2,3-triazol-1-yl)pyrrolidine-2-carboxylic Acid (**2o**).



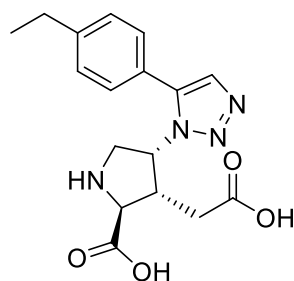
Prepared according to general procedure A and B. The product was isolated by preparative HPLC: Rt: 10.0 min; flow: 20 mL min⁻¹; gradient 0–50% B (25 min); λ = 210 nm. The product **2o** was obtained as a white solid in 30% yield, over two steps, C4 epimer <1%. ¹H NMR (600 MHz, D₂O): δ 7.97 (s, 1H), 7.53 (t, J = 7.7 Hz, 1H), 7.19 (d, J = 7.9 Hz, 1H), 7.11–7.03 (m, 2H), 5.75 (m, 1H), 4.23 (m, 3H), 3.89 (s, 3H), 3.31 (s, 1H), 2.85 (d, J = 17.8 Hz, 1H), 1.75 (dt, J = 28.4, 13.6 Hz, 1H). ¹³C NMR (151 MHz, D₂O): δ 173.3, 170.3, 159.3, 130.9, 130.8, 126.1, 122.1, 121.9, 116.3, 114.9, 114.8, 55.9, 55.8, 51.0, 30.8 ppm. UPLC-MS (*m/z*) calcd for C₁₆H₁₈N₄O₅⁺ [M + H]⁺ 347.1, found 347.4.

(2*S*,3*R*,4*R*)-4-(4/5-(3-Aminophenyl)-1*H*-1,2,3-triazol-1-yl)-3-(carboxymethyl)pyrrolidine-2-carboxylic Acid (**2p**).



Prepared according to general procedure A and B. The product was isolated by preparative HPLC: Rt: 5.2 min; flow: 20 mL min⁻¹; gradient 0–50% B (25 min); λ = 210 nm. Pale yellow solid, yield 13% (4-phenyl-triazol:5-phenyl-triazol = 2:1). ¹H NMR (400 MHz, MeOD): δ 7.83 (s, 1H), 7.53–7.48 (m, 1H), 7.29–7.23 (m, 3H), 5.62 (t, J = 6.1 Hz, 1H), 4.58 (d, J = 11.7 Hz, 1H), 4.05 (dd, J = 13.2, 6.1 Hz, 1H), 3.95 (d, J = 13.3 Hz, 1H), 3.19 (m, 1H), 2.73 (dd, J = 17.8, 4.0 Hz, 1H), 1.67 (dd, J = 17.8, 10.5 Hz, 1H). ¹³C NMR (101 MHz, MeOD): δ 170.4, 168.5, 139.6, 132.8, 130.4, 126.8, 123.9, 120.6, 119.5, 62.1, 58.9, 50.7, 43.5, 30.4. C₁₅H₁₇N₅O₄. UPLC-MS (*m/z*) calcd for C₁₅H₁₈N₅O₄⁺ [M + H]⁺ 332.1, found 332.1.

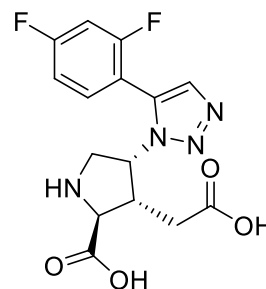
(2*S*,3*R*,4*R*)-3-(Carboxymethyl)-4-(5-(4-ethylphenyl)-1*H*-1,2,3-triazol-1-yl)pyrrolidine-2-carboxylic Acid (**2q**).



Prepared according to general procedure A and B. The product was isolated by preparative HPLC: Rt: 12.4 min; flow: 20 mL

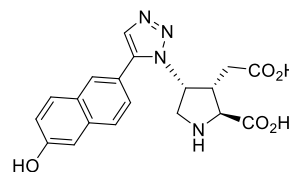
min⁻¹; gradient 0–50% B (25 min); λ = 210 nm. The product **2q** was obtained as a white solid in 33% yield over two steps, C4 epimer <1%. ¹H NMR (600 MHz, D₂O): δ 7.79 (s, 1H), 7.39 (d, J = 7.9 Hz, 2H), 7.36–7.29 (m, 2H), 5.46 (t, J = 6.0 Hz, 1H), 4.27 (d, J = 11.1 Hz, 1H), 3.97 (dd, J = 13.2, 6.1 Hz, 1H), 3.85 (d, J = 13.0 Hz, 1H), 3.00 (m, 1H), 2.70–2.59 (m, 3H), 1.60 (dd, J = 16.9, 11.1 Hz, 1H), 1.19 (t, J = 7.5 Hz, 3H). ¹³C NMR (151 MHz, D₂O): δ 177.29, 173.23, 147.06, 140.39, 132.82, 129.39, 128.66, 122.50, 64.51, 59.09, 50.84, 45.64, 34.65, 28.14, 14.82. UPLC-MS (*m/z*) calcd for C₁₇H₂₀N₄O₄⁺ [M + H]⁺ 345.2, found 345.4.

(2*S*,3*R*,4*R*)-3-(Carboxymethyl)-4-(5-(2,4-difluorophenyl)-1*H*-1,2,3-triazol-1-yl)pyrrolidine-2-carboxylic Acid (**2r**).



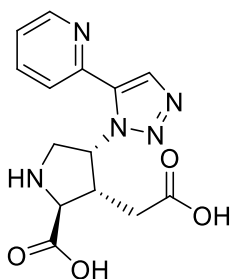
Prepared according to general procedure A and B. The product was isolated by preparative HPLC: Rt: 8.2 min; flow: 20 mL min⁻¹; gradient 0–50% B (25 min); λ = 210 nm. The product **2r** was obtained as a white solid in 37% yield over two steps, C4 epimer <1%. ¹H NMR (400 MHz, MeOD): δ 7.83 (s, 1H), 7.41 (m, 1H), 7.09 (m, 2H), 5.37 (t, J = 6.2 Hz, 1H), 4.58 (d, J = 11.8 Hz, 1H), 4.03 (dd, J = 13.3, 6.3 Hz, 1H), 3.83 (d, J = 13.2 Hz, 1H), 3.14 (m, 1H), 2.82–2.74 (m, 1H), 1.63 (dd, J = 18.0, 10.9 Hz, 1H). ¹³C NMR (101 MHz, MeOD): δ 171.6, 168.7, 133.8, 133.5, 133.0, 112.2, 104.5, 62.3, 59.2, 50.7, 43.6, 30.4. UPLC-MS (*m/z*) calcd for C₁₅H₁₄F₂N₄O₄⁺ [M + H]⁺ 353.1, found 353.3.

(2*S*,3*R*,4*R*)-3-(Carboxymethyl)-4-(5-(6-hydroxynaphthalen-2-yl)-1*H*-1,2,3-triazol-1-yl)pyrrolidine-2-carboxylic Acid (**2s**, LBG20304).



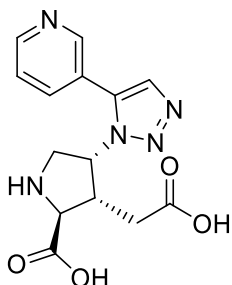
Carried out according to general procedure B and product **2s** isolated by preparative HPLC: Rt: 12.6 min; flow: 20 mL min⁻¹; isocratic 0–50%B (25 min); λ = 210 nm. White solid (14 mg, 58%). Contains ~2% of the C4-epimer. Major diastereomer: ¹H NMR (600 MHz, D₂O) δ 8.00 (s, 1H), 7.94 (m, 3H), 7.49 (d, J = 8.6 Hz, 1H), 7.37 (d, J = 2.4 Hz, 1H), 7.30 (dd, J = 8.6, 2.5 Hz, 1H), 5.79 (t, J = 5.2 Hz, 1H), 4.40 (dd, J = 11.6 Hz, 1H), 4.23–4.15 (m, 2H), 3.18–3.08 (m, 1H), 2.87 (dd, J = 18.1, 3.5 Hz, 1H), 1.79 (ddd, J = 18.1, 10.9, 1.3 Hz, 1H). ¹³C NMR (151 MHz, D₂O) δ 173.3, 171.8, 154.9, 140.5, 134.9, 133.1, 130.5, 129.1, 128.0, 127.5, 126.3, 119.9, 119.2, 109.3, 63.2, 59.0, 50.6, 44.0, 31.2. UPLC-MS (*m/z*) calcd for C₁₉H₁₈N₄O₅⁺ [M + H]⁺, 383.2; found, 383.6.

(2*S*,3*R*,4*R*)-3-(Carboxymethyl)-4-(5-(pyridin-2-yl)-1*H*-1,2,3-triazol-1-yl)pyrrolidine-2-carboxylic Acid (**2t**).



Prepared according to general procedure A and B. The product was isolated by preparative HPLC: Rt: 7.2 min; flow: 20 mL min⁻¹; gradient 0–50% B (25 min); $\lambda = 210$ nm. The product was obtained as a white solid in 8% yield over two steps, C4 epimer <1%. ¹H NMR (600 MHz, D₂O): δ 8.59 (s, 1H), 8.10 (m, 1H), 8.00 (m, 1H), 7.71 (m, 1H), 7.53 (m, 1H), 6.18 (m, 1H), 4.05 (m, 2H), 3.08 (m, 1H), 2.69 (m, 1H), 1.53 (m, 1H). ¹³C NMR (151 MHz, D₂O) δ 177.02, 172.99, 150.01, 148.51, 138.15, 136.99, 133.64, 124.48, 122.41, 64.29, 59.43, 50.67, 45.70, 34.53. UPLC-MS (*m/z*) calcd for C₁₄H₁₅N₅O₄⁺ [M + H]⁺ 318.1, found 318.3.

(2*S*,3*R*,4*R*)-3-(Carboxymethyl)-4-(5-(pyridin-3-yl)-1*H*-1,2,3-triazol-1-yl)pyrrolidine-2-carboxylic Acid (**2u**).



Prepared according to general procedure A and B. The product was isolated by preparative HPLC: Rt: 7.6 min; flow: 20 mL min⁻¹; gradient 0–50% B (25 min); $\lambda = 210$ nm. The product **2u** was obtained as a white solid in 48% yield, over two steps, C4 epimer <1%. ¹H NMR (600 MHz, D₂O): δ 8.97 (s, 1H), 8.88 (m, 1H), 8.66 (d, *J* = 7.4 Hz, 1H), 8.16 (m, 1H), 8.06 (m, 1H), 5.59 (m, 1H), 4.50 (m, 1H), 4.07 (m, 2H), 3.16 (m, 1H), 2.81 (d, *J* = 18.1 Hz, 1H), 1.68 (m, 1H). ¹³C NMR (151 MHz, D₂O): δ 173.6, 170.4, 147.0, 142.6, 141.3, 135.0, 133.6, 128.0, 125.8, 62.6, 59.3, 50.7, 43.55, 30.9. UPLC-MS (*m/z*) calcd for C₁₄H₁₅N₅O₄⁺ [M + H]⁺ 318.1, found 318.3.

Binding Affinities. Ligand binding affinities for native AMPA, KA, and NMDA receptors in rat cortical synaptosomes were determined as previously described using [³H]-AMPA, [³H]-KA, and [³H]-CGP 39653, respectively.²⁸ CPM values were fitted by nonlinear regression using GraphPad Prism 7.0 (GraphPad Software, San Diego, CA).

Binding affinities for GluK1-3 and GluA2 were determined following the procedure published in Demmer et al.²⁹ Binding affinities for homomeric GluK5 were carried out according to Møllerud et al.³⁰

Electrophysiology (HEK293T cells). HEK293T cells were maintained in MEM containing glutamine and supplemented with 10% fetal bovine serum (Gibco). Cells were plated at low density (1.6 × 10⁴ cells/ml) on poly-D-lysine-coated, 35 mm, plastic dishes and were transiently transfected 48 h later using the calcium phosphate technique, as previously described.²⁵

Experiments were performed 48–72 h after washing transfection media. Agonist was rapidly applied to outside-out patches excised from transfected cells using a piezoelectric stack (Physik Instrumente).

Solution exchange (10–90% rise time of 250–350 μ s) was determined by measuring the liquid junction current at the end of an experiment. All recordings were performed using an Axopatch 200B (Molecular Devices) with thick-walled, borosilicate glass pipettes (3–6 M Ω) coated with dental wax to reduce electrical noise. Series resistance (3–12 M Ω) was compensated by 95%. Data acquisition was performed using pClamp10 software (Molecular Devices) and was tabulated using Excel (Microsoft Corp.). All experiments were performed at room temperature.

All chemicals were purchased from Sigma-Aldrich, unless otherwise indicated. The external solution contained (in mM) 150 NaCl, 5 HEPES, and 0.1 CaCl₂, at pH 7.3–7.4. The internal solution contained (mM) 115 NaCl, 10 NaF, 5 HEPES, 5 Na₄BAPTA (Life Technologies), 1 MgCl₂, 0.5 CaCl₂, and 10 Na₂ATP, pH 7.3–7.4. The osmotic pressure of these solutions was adjusted to 295–300 mOsm with sucrose.

Concentrated (10 ×) agonist stock solutions were prepared by dissolving Glu in the appropriate external solution and adjusting the pH to 7.3–7.4 and were stored frozen at –20 °C. Stocks were thawed on the day of the experiment and used to prepare agonist-containing external solutions.

Electrophysiology in Slices. All experiments were conducted in strict compliance with the European Union recommendations (2013/63/EU) and were approved by the French Ministry of Higher Education, Research and Innovation and the local ethical committee of the University of Bordeaux (APAFIS #37890–2022070114075354).

To perform electrophysiology on hippocampal slices, we anesthetized mice of both sexes (>3-week-old) using an intraperitoneal injection of a mixture containing ketamine (100 mg/kg) and xylazine (20 mg/kg) diluted in saline. Subsequently, the mice underwent transcardial perfusion with an ice-cold cutting solution composed of the following concentrations (in mM): 75 Sucrose, 87 NaCl, 2.5 KCl, 1.25 NaH₂PO₄, 25 NaHCO₃, 25 Glucose, 0.5 CaCl₂, and 7 MgCl₂, with a pH of 7.4 and an osmolarity of 315 mOsm. After decapitation, the mouse's head was immersed in ice-cold cutting solution, and the brain was removed and sliced parasagittally (300 μ m) using a vibratome (model VT1200S, Leica Microsystems). The slices were then allowed to recover for 20 min at 32 °C in artificial cerebrospinal fluid (aCSF) consisting of the following concentrations (in mM): 125 NaCl, 2.5 KCl, 1.25 NaH₂PO₄, 26 NaHCO₃, 10 Glucose, 2.8 Pyruvic acid, 2.3 CaCl₂, and 1.3 MgCl₂, with a pH of 7.4 and an osmolarity of 305 mOsm. Both the cutting solution and aCSF were saturated with carbogen (95% O₂ and 5% CO₂).

In the electrophysiology recording chamber, the slices were submerged and continuously perfused with carbogenated aCSF at room temperature. Whole-cell patch clamp recordings were conducted on CA3 pyramidal cells with the assistance of a differential interference contrast microscope. Recordings were carried out using silver-chloride electrodes enclosed by borosilicate glass capillaries, connected to a HEKA EPC10 amplifier (Lambrecht, Germany). The patch-pipettes were filled with an intracellular solution containing (in mM): 125 Cesium-Methanesulfonate, 2 MgCl₂, 4 NaCl, 5 phosphocreatine, 4 Na₂ATP, 10 EGTA, 10 HEPES with a pH adjusted to 7.3 using CsOH, and an osmolarity of 300 mOsm. During recordings, 50 μ M D-APV, 20 μ M LY-307070 and 10 μ M Bicuculline, were present to block respectively NMDA, AMPA and GABA_A receptors. Data analysis was performed using IGOR PRO 6.3 or 9.0 (Wavemetrics) with the Neuromatic extension³¹ and Prism (GraphPad, San Diego, CA, USA). Data values are given as mean \pm SEM.

Kinetics. For the interrogation of gating properties of kainate receptors, a single voltage step to –100 mV along with 1 ms application of L-Glu was applied to measure the deactivation time constant. Deactivation kinetics were calculated using a mono, double or triple exponential function as the following:

Mono exponential function

$$t_{\text{deact}} = -tA$$

Double exponential function

$$t_{w,deact} = t_1 \left(\frac{A_1}{A_1 + A_2} \right) + t_2 \left(\frac{A_2}{A_1 + A_2} \right)$$

Triple exponential function

$$t_{w,deact} = t_1 \left(\frac{A_1}{A_1 + A_2 + A_3} \right) + t_2 \left(\frac{A_2}{A_1 + A_2 + A_3} \right) + t_3 \left(\frac{A_3}{A_1 + A_2 + A_3} \right)$$

Where A and t are the amplitude and time constant components.

Statistics. Shapiro-Wilk test was used to test the normality for all data sets. Paired sample t test, unpaired Welch t test and Mann–Whitney test were used to do hypothesis contrast for normal and non-normal distributed data, respectively.

Tw (ms)	Average	SEM	n	p-value
GluK2	3.5	1.1	11	
GluK2/K5 (1mM L-Glu)	32.8	5	10	<0.001

GluK2/K5 (1mM L-Glu)	38.7	7.7	5	0.8
GluK2/K5 (1mM L-Glu + 10 μM LBG 20304)	35.1	9.8	5	

Normalized peak amplitude				
	Average	SEM	n	p-value
1 mM L-Glu	1	-	5	0.7
1 mM L-Glu + 10 μM LBG 20304	1.01	0.03	5	

■ ASSOCIATED CONTENT

SI Supporting Information

The Supporting Information is available free of charge at <https://pubs.acs.org/doi/10.1021/acs.jmedchem.4c01311>.

Molecular formula strings (CSV)
 GluK5 homology model with LBG20304 (PDB)
 GluK5 homology model with DA (PDB)
¹H and ¹³C NMR and analytical HPLC traces of LBG20304 (2s), analytical HPLC traces of 2a–c, description of the method for the MD simulation, including Figures S1–S3 showing these and the results thereof (PDF)

■ AUTHOR INFORMATION

Corresponding Author

Lennart Bunch – Department of Drug Design and Pharmacology, Faculty of Health and Medical Sciences, University of Copenhagen, 2100 Copenhagen, Denmark; orcid.org/0000-0002-0180-4639; Email: lebu@sund.ku.dk

Authors

Silke Buschbom-Helmke – Department of Drug Design and Pharmacology, Faculty of Health and Medical Sciences, University of Copenhagen, 2100 Copenhagen, Denmark
Pengfei Wang – Department of Drug Design and Pharmacology, Faculty of Health and Medical Sciences, University of Copenhagen, 2100 Copenhagen, Denmark

Anna Alcaide – Department of Drug Design and Pharmacology, Faculty of Health and Medical Sciences, University of Copenhagen, 2100 Copenhagen, Denmark

Federico Miguez-Cabello – Department of Pharmacology & Therapeutics, Faculty of Medicine, McGill University, H3G 0B1 Montréal, Canada

Mario Carta – Interdisciplinary Institute for Neuroscience, CNRS UMR 5297, University of Bordeaux, F-33000 Bordeaux, France

Julio S. Viotti – Interdisciplinary Institute for Neuroscience, CNRS UMR 5297, University of Bordeaux, F-33000 Bordeaux, France

Birgitte Nielsen – Department of Drug Design and Pharmacology, Faculty of Health and Medical Sciences, University of Copenhagen, 2100 Copenhagen, Denmark

Christophe Mulle – Interdisciplinary Institute for Neuroscience, CNRS UMR 5297, University of Bordeaux, F-33000 Bordeaux, France

Derek Bowie – Department of Pharmacology & Therapeutics, Faculty of Medicine, McGill University, H3G 0B1 Montréal, Canada

Flemming Steen Jørgensen – Department of Drug Design and Pharmacology, Faculty of Health and Medical Sciences, University of Copenhagen, 2100 Copenhagen, Denmark; orcid.org/0000-0001-8040-2998

Darryl S. Pickering – Department of Drug Design and Pharmacology, Faculty of Health and Medical Sciences, University of Copenhagen, 2100 Copenhagen, Denmark

Complete contact information is available at: <https://pubs.acs.org/doi/10.1021/acs.jmedchem.4c01311>

Notes

The authors declare no competing financial interest.

■ ACKNOWLEDGMENTS

The authors thank the Lundbeck Foundation for financial support. J.S.V., M.C., and C.M. were supported by the French Centre National de la Recherche Scientifique and by ANR Grant Target-KAREP.

■ ABBREVIATIONS USED

AMPA, α-amino-3-hydroxy-5-methyl-4-isoxazolepropionic acid; CPM, counts per minute; DA, domoic acid; Glu, glutamate; iGluRs, ionotropic Glu receptors; KA, kainic acid; LBD, ligand binding domain; mGluRs, metabotropic Glu receptors; NMDA, N-methyl D-aspartate; SAR, structure–activity relationship; TBAF, tetra-*N*-butylammonium fluoride

■ REFERENCES

- Stawski, P.; Janovjak, H.; Trauner, D. Pharmacology of Ionotropic Glutamate Receptors: A Structural Perspective. *Bioorg. Med. Chem.* **2010**, *18* (22), 7759–7772.
- Khanra, N.; Brown, P. M. G. E.; Perozzo, A. M.; Bowie, D.; Meyerson, J. R. Architecture and Structural Dynamics of the Heteromeric GluK2/K5 Kainate Receptor. *eLife* **2021**, *10*, e66097 DOI: [10.7554/eLife.66097](https://doi.org/10.7554/eLife.66097).
- Stensbøl, T. B.; Borre, L.; Johansen, T. N.; Egebjerg, J.; Madsen, U.; Ebert, B.; Krosgaard-Larsen, P. Resolution, Absolute Stereochemistry and Molecular Pharmacology of the Enantiomers of ATPA. *Eur. J. Pharmacol.* **1999**, *380* (2–3), 153–162.
- Weiss, B.; Alt, A.; Ogden, A. M.; Gates, M.; Dieckman, D. K.; Clemens-smith, A.; Ho, K. H.; Jarvie, K.; Rizkalla, G.; Wright, R. a; Calligaro, D. O.; Schoepp, D.; Mattiuz, E. L.; Stratford, R. E.; Johnson,

- B.; Salhoff, C.; Katofiasc, M.; Phebus, L. a; Schenck, K.; Cohen, M.; Filla, S. a; Ornstein, P. L.; Johnson, K. W.; Bleakman, D. Pharmacological Characterization of the Competitive GLU K5 Receptor Antagonist Decahydroisoquinoline LY466195 in Vitro and in Vivo. *J. Pharmacol. Exp. Ther.* **2006**, *318* (2), 772–781.
- (5) Dolman, N. P.; More, J. C. A.; Alt, A.; Knauss, J. L.; Pentikäinen, O. T.; Glasser, C. R.; Bleakman, D.; Mayer, M. L.; Collingridge, G. L.; Jane, D. E. Synthesis and Pharmacological Characterization of N3-Substituted Willardiine Derivatives: Role of the Substituent at the 5-Position of the Uracil Ring in the Development of Highly Potent and Selective GLUK5 Kainate Receptor Antagonists. *J. Med. Chem.* **2007**, *50* (7), 1558–1570.
- (6) Valgeirsson, J.; Nielsen, E.; Peters, D.; Mathiesen, C.; Kristensen, A. S.; Madsen, U. Bioisosteric Modifications of 2-Arylureidobenzoic Acids: Selective Noncompetitive Antagonists for the Homomeric Kainate Receptor Subtype GluR5. *J. Med. Chem.* **2004**, *47* (27), 6948–6957.
- (7) Møllerud, S.; Pinto, A.; Marconi, L.; Frydenvang, K.; Thorsen, T. S.; Laulumaa, S.; Venskutonyte, R.; Winther, S.; Moral, A. M. C.; Tamborini, L.; Conti, P.; Pickering, D. S.; Kastrup, J. S. Structure and Affinity of Two Bicyclic Glutamate Analogues at AMPA and Kainate Receptors. *ACS Chem. Neurosci.* **2017**, *8* (9), 2056–2064.
- (8) Conti, P.; de Amici, M.; de Sarro, G.; Rizzo, M.; Stensbøl, T. B.; Bräuner-Osborne, H.; Madsen, U.; Toma, L.; de Micheli, C. Synthesis and Enantiopharmacology of New AMPA-Kainate Receptor Agonists. *J. Med. Chem.* **1999**, *42* (20), 4099–4107.
- (9) Poulie, C. B. M.; Larsen, Y.; Leteneur, C.; Barthet, G.; Bjorn-Yoshimoto, W. E.; Malhaire, F.; Nielsen, B.; Pin, J. P.; Mulle, C.; Pickering, D. S.; Bunch, L. (S)-2-Mercaptohistidine: A First Selective Orthosteric GluK3 Antagonist. *ACS Chem. Neurosci.* **2022**, *13*, 1580–1587.
- (10) Møllerud, S.; Frydenvang, K.; Pickering, D. S.; Kastrup, J. S. Lessons from Crystal Structures of Kainate Receptors. *Neuropharmacology* **2017**, *112*, 16–28.
- (11) Meyerson, J. R.; Kumar, J.; Chittori, S.; Rao, P.; Pierson, J.; Bartesaghi, A.; Mayer, M. L.; Subramaniam, S. Structural Mechanism of Glutamate Receptor Activation and Desensitization. *Nature* **2014**, *514*:7522 **2014**, *514* (7522), 328–334.
- (12) Murakami, S.; Takemoto, T.; Shimizu, Z. Studies on Active Ingredients of Seaweed (1st Report). *J. Pharm. Soc. Jpn.* **1953**, *73*, 1026–1028.
- (13) Sagot, E.; Pickering, D. S.; Pu, X.; Umberti, M.; Stensbøl, T. B.; Nielsen, B.; Chapelet, M.; Bolte, J.; Gefflaut, T.; Bunch, L. Chemo-Enzymatic Synthesis of a Series of 2,4-Syn-Functionalized (S)-Glutamate Analogues: New Insight into the Structure-Activity Relation of Ionotropic Glutamate Receptor Subtypes 5, 6, and 7. *J. Med. Chem.* **2008**, *51* (14), 4093–4103.
- (14) Sawant, P. M.; Weare, B. A.; Holland, P. T.; Selwood, A. I.; King, K. L.; Mikulski, C. M.; Doucette, G. J.; Mountfort, D. O.; Kerr, D. S. Isodomoic Acids A and C Exhibit Low KA Receptor Affinity and Reduced in Vitro Potency Relative to Domoic Acid in Region CA1 of Rat Hippocampus. *Toxicol.* **2007**, *50* (5), 627–638.
- (15) Baldwin, J. E.; Fryer, A. M.; Pritchard, G. J. Parallel Synthesis of Novel Heteroaromatic Acromelic Acid Analogues from Kainic Acid. *J. Org. Chem.* **2001**, *66* (8), 2588–2596.
- (16) Kwak, S.; Aizawa, H.; Ishida, M.; Shinozaki, H. New, Potent Kainate Derivatives: Comparison of Their Affinity for [³H]Kainate and [³H]AMPA Binding Sites. *Neurosci. Lett.* **1992**, *139* (1), 114–117.
- (17) Hampson, D. R.; Huang, X.-p.; Wells, J. W.; Walter, J. A.; Wright, J. L. C. Interaction of Domoic Acid and Several Derivatives with Kainic Acid and AMPA Binding Sites in Rat Brain. *Eur. J. Pharmacol.* **1992**, *218* (1), 1–8.
- (18) Hald, H.; Naur, P.; Pickering, D. S.; Sprogøe, D.; Madsen, U.; Timmermann, D. B.; Ahring, P. K.; Liljefors, T.; Schousboe, A.; Egebjerg, J.; Gajhede, M.; Kastrup, J. S. Partial Agonism and Antagonism of the Ionotropic Glutamate Receptor IGLuR5: Structures of the Ligand-Binding Core in Complex with Domoic Acid and 2-Amino-3-[5-Tert-Butyl-3-(Phosphonomethoxy)-4-Isoxazolyl]-Propionic Acid. *J. Biol. Chem.* **2007**, *282* (35), 25726–25736.
- (19) Nanao, M. H.; Green, T.; Stern-Bach, Y.; Heinemann, S. F.; Choe, S. Structure of the Kainate Receptor Subunit GluR6 Agonist-Binding Domain Complexed with Domoic Acid. *Proc. Natl. Acad. Sci. U. S. A.* **2005**, *102* (5), 1708–1713.
- (20) Karppanen, E. J.; Koskinen, A. M. P. The 9-Phenyl-9-Fluorenyl Group for Nitrogen Protection in Enantiospecific Synthesis. *Molecules* **2010**, *15* (9), 6512–6547.
- (21) Zanato, C.; Watson, S.; Bewick, G. S.; Harrison, W. T. A.; Zanda, M. Synthesis and Biological Evaluation of (–)-Kainic Acid Analogues as Phospholipase D-Coupled Metabotropic Glutamate Receptor Ligands. *Org. Biomol. Chem.* **2014**, *12* (47), 9638–9643.
- (22) Boren, B. C.; Narayan, S.; Rasmussen, L. K.; Zhang, L.; Zhao, H.; Lin, Z.; Jia, G.; Fokin, V. v. Ruthenium-Catalyzed Azide-Alkyne Cycloaddition: Scope and Mechanism. *J. Am. Chem. Soc.* **2008**, *130* (28), 8923–8930.
- (23) Pradere, U.; Roy, V.; McBrayer, T. R.; Schinazi, R. F.; Agrofoglio, L. A. Preparation of Ribavirin Analogues by Copper- and Ruthenium-Catalyzed Azide-Alkyne 1,3-Dipolar Cycloaddition. *Tetrahedron* **2008**, *64* (38), 9044–9051.
- (24) Masternak, M.; Koch, A.; Laulumaa, S.; Tapken, D.; Hollmann, M.; Jørgensen, F. S.; Kastrup, J. S. Differences between the GluD1 and GluD2 Receptors Revealed by GluD1 X-Ray Crystallography, Binding Studies and Molecular Dynamics. *FEBS J.* **2023**, *290* (15), 3781–3801.
- (25) Brown, P. M. G. E.; Arousseau, M. R. P.; Musgaard, M.; Biggin, P. C.; Bowie, D. Kainate Receptor Pore-Forming and Auxiliary Subunits Regulate Channel Block by a Novel Mechanism. *J. Physiol.* **2016**, *594* (7), 1821–1840.
- (26) Barberis, A.; Sachidhanandam, S.; Mulle, C. GluR6/KA2 Kainate Receptors Mediate Slow-Deactivating Currents. *J. Neurosci.* **2008**, *28* (25), 6402–6406.
- (27) Mulle, C.; Crépel, V. Regulation and Dysregulation of Neuronal Circuits by KARs. *Neuropharmacology* **2021**, *197*, 108699.
- (28) Assaf, Z.; Larsen, A. P.; Venskutonytė, R.; Han, L.; Abrahamson, B.; Nielsen, B.; Gajhede, M.; Kastrup, J. S.; Jensen, A. A.; Pickering, D. S.; Frydenvang, K.; Gefflaut, T.; Bunch, L. Chemoenzymatic Synthesis of New 2,4-Syn-Functionalized (S)-Glutamate Analogues and Structure-Activity Relationship Studies at Ionotropic Glutamate Receptors and Excitatory Amino Acid Transporters. *J. Med. Chem.* **2013**, *56* (4), 1614–1628.
- (29) Demmer, C. S.; Rombach, D.; Liu, N.; Nielsen, B.; Pickering, D. S.; Bunch, L. Revisiting the Quinoxalinedione Scaffold in the Construction of New Ligands for the Ionotropic Glutamate Receptors. *ACS Chem. Neurosci.* **2017**, *8* (11), 2477–2495.
- (30) Møllerud, S.; Kastrup, J. S.; Pickering, D. S. A Pharmacological Profile of the High-Affinity GluK5 Kainate Receptor. *Eur. J. Pharmacol.* **2016**, *788*, 315–320.
- (31) Rothman, J. S.; Silver, R. A. Neuromatic: An Integrated Open-Source Software Toolkit for Acquisition, Analysis and Simulation of Electrophysiological Data. *Front. Neuroinform.* **2018**, *12*, 335195.